EXPERIMENTAL EVALUATION OF WIRE MESH FOR DESIGN AS A BEARING DAMPER

A Thesis

by

VIVEK VAIBHAV CHOUDHRY

Submitted to the Office of Graduate Studies of
Texas A&M University
in partial fulfillment of the requirements for the degree of

MASTER OF SCIENCE

August 2004

Major Subject: Mechanical Engineering

EXPERIMENTAL EVALUATION OF WIRE MESH FOR DESIGN AS A BEARING DAMPER

A Thesis

by

VIVEK VAIBHAV CHOUDHRY

Submitted to the Office of Graduate Studies of
Texas A&M University
in partial fulfillment of the requirements for the degree of

MASTER OF SCIENCE

Approved as to style and content by:

John M. Vance (Chair of Committee)	Alan Palazzolo (Member)
Maurice Rahe (Member)	Dennis O'Neal (Head of Department)

August 2004

Major Subject: Mechanical Engineering

ABSTRACT

Experimental Evaluation of Wire Mesh for Design as a Bearing Damper. (August 2004)

Vivek Vaibhav Choudhry, B.S., Regional Engineering College, Allahabad, India

Chair of Advisory Committee: Dr. John M. Vance

Wire mesh vibration dampers have been the subject of some very encouraging experiments at the Texas A&M Turbomachinery laboratories for the past several years and have emerged as an excellent replacement for squeeze film dampers. Their capability to provide damping for a wide range of temperatures (even cryogenic), fluid free operation and ability to perform even when soaked with lubricants makes them a suitable option as a bearing damper. Experiments were conducted to investigate the effect of design parameters like axial thickness and axial compression that influence the characteristics of wire mesh as a bearing damper. Two groups of wire mesh were tested to show that the stiffness and damping are directly proportional to the axial thickness, if all the other parameters are kept constant. Tests on four wire mesh donuts of different radial thickness showed that stiffness and damping vary inversely with radial thickness. Rigorous tests were also conducted to quantify the effects of axial compression, radial interference and displacement amplitude on stiffness and damping of the wire mesh. Another novel kind of mesh damper tested was comprised of two small segments instead of a whole donut. The results showed that wire mesh exhibited good damping characteristics even when used in small segments. Empirical expressions were developed using MathCAD™ worksheets, and an existing Excel™ design worksheet was modified to include these factors. The effect of frequency variation was also included to give a comprehensive design tool for wire mesh. A new design worksheet was developed that can predict rotordynamic coefficients for a wire mesh bearing damper having a different size as well as different installation and operational conditions.

To my Family and Friends.

ACKNOWLEDGMENTS

I would like to express my sincere appreciation to the chair of my advisory committee, Dr. John M. Vance for his guidance and support. He provided me immense support and an excellent opportunity to work on the wire mesh bearing dampers, which proved to be exciting and challenging in the turbomachinery field. His exhaustive knowledge of turbomachinery and engineering in general has been a great source of learning to me. Without his patience, encouragement and dedication to my research, the completion of this thesis would have been difficult.

Sincere appreciation is extended to Dr. Alan Palazzolo and Dr. Maurice Rahe for their participation on the graduate committee and their understanding nature. I am also thankful to Dr. Dara Childs for all his support and advice during the course of my research.

I am grateful to Bugra Ertas, Bharathwaj Kannan and Anand Srinivasan for helping me understand the fundamentals of mechanical engineering and turbomachinery. I must also thank Ahmed Gamal, Mohsin Jafri and Rahul Kar for making those long hours spent at Turbomachinery Laboratory so much fun.

NOMENCLATURE

AC	Axial compression
Amp	Displacement Amplitude
AT	Axial Thickness
C	Damping (Viscous) Coefficient
Const1	Constant used in the stiffness formula
Const2	Constant used in the damping formula
E'	Equivalent Young's modulus.
F	Force in the X direction
H	Hysteretic damping coefficient
K	Stiffness Coefficient
K_{xx}	Direct stiffness in X direction
K_{yy}	Direct stiffness in Y direction
L	Axial length
om, Ω	Frequency
Ri	Inner Radius
Ro	Outer Radius
RI	Radial Interference
RT	Radial Thickness
t	time
X	Displacement in X direction
β	Loss Coefficient
δ	Logarithmic decrement
ϕ	Phase
θ	Angle of the smallest unit taken in the donut
ω	Frequency
ω_n	Natural frequency

TABLE OF CONTENTS

Page

LIST OF FIGURES

LIST OF TABLES

INTRODUCTION

To minimize the detrimental effect of vibration in machinery, it is always desirable to keep vibration amplitudes as low as possible. In machines with rolling-element bearings, dynamic loads should also be minimized to maximize bearing life. Vibration in a turbo-machine can result from various causes like imbalance, misalignment, flow pulsation, resonance and destabilizing forces. The large number of sources of vibration makes it impractical to contain vibration by minimizing the source always. An alternative approach is to channel the vibration energy to where it can be absorbed or dissipated safely. One of the options for such an approach is a bearing damper.

For the past three decades squeeze film dampers (SFD) have been used extensively in aircraft engines, and in more than 300 industrial compressors, for providing damping at bearing locations. The high damping forces of the SFD, combined with low support stiffness, decrease the vibration levels and dynamic loads, and improve rotordynamic stability. However, despite its useful characteristics, the SFD has some inherent disadvantages. Damping being dependent on the viscosity of oil, the performance of the SFD decreases considerably at very high and very low temperatures. The SFD cannot sustain high vibration amplitudes, such as from large imbalance. Air ingestion into the SFD creates bubbles in the oil and makes its performance unpredictable. Dependence on oil also makes it less attractive especially with the growing interest towards oil-free machinery.

Over the past few years wire mesh bearing dampers have emerged in our laboratory tests as a superior alternative to the SFD. Wire mesh not only provides comparative performance advantages over the SFD, but also maintains its characteristics

---

This thesis follows the style and format of the ASME Journal of Engineering for Gas Turbines and Power.

under adverse conditions. The wire mesh bearing damper design under investigation is a short hollow cylinder made out of woven metal strands. Experiments conducted so far in the turbomachinery laboratory have confirmed (as originally shown by Wang Xin and Zhu [1] that it can control more rotor imbalance than a SFD. It has retained most of its damping characteristics when tested at high temperature (212 F) as well as at cryogenic (liquid nitrogen) temperature. It has also shown the same unchanged performance whether dry or wet (oil-lubricated). An application to a turboprop aircraft engine has been demonstrated on a rotordynamic test stand. Low temperature shaker tests and computer simulations of the pump rotordynamics have demonstrated application to cryogenic turbo pumps. The reliability (life) of copper mesh dampers was demonstrated by a test under practical vibration conditions for a year. The mesh donuts, as tested, are available at low cost.

A design analysis model for the stiffness and damping coefficients of the wire mesh bearing damper is the subject of this thesis. Experiments conducted by Al-Khateeb [2] showed a change of the stiffness and damping coefficients with frequency and vibration amplitude. Prediction equations used by Zarzour [3] give the coefficients for donuts of different size but under similar test conditions and wire mesh material. Al-Khateeb showed that these equations would have to be modified to include the effect of other design parameters and test conditions.

RESEARCH OBJECTIVES, NEED, AND LITERATURE REVIEW

Research Objectives

The primary objective of this research is to study and quantify the characteristics of wire mesh bearing dampers under different design, installation and operational conditions. A standard engineering guideline in the form of an Excel sheet is sought that could be used in designing and optimizing the wire mesh as bearing dampers. This is to be attained by accomplishment of the following tasks:

- To conduct experiments that will determine the effect of design factors like axial thickness and radial thickness on wire mesh stiffness and damping properties.
- To quantify the effects of axial thickness, radial thickness, axial compression, radial interference, and dynamic strain on the rotordynamic characteristics of the wire mesh, based on experiments by previous investigators.
- To modify and improve the design guidelines presented by Al-Khateeb [2], to include the effects of variation of different design, installation and operational parameters, and to implement the equations into an Excel^{TM} workbook.

Need Statement

The demonstrated ability to perform well under diverse conditions of temperature, oil free operation, and demonstrated reliability over a one year test makes wire mesh an excellent bearing damper material. Despite the availability of wire mesh, research in the area of its utilization as a bearing damper has been very limited. Currently, an engineer would find difficulty when trying to design a wire mesh damper for real turbomachinery applications. One of the reasons for this is the lack of knowledge about the stiffness and damping behavior of wire mesh when subject to variable design parameters like axial and radial thickness of the wire mesh. The quantitative effects of various design, installation and operational parameters on the characteristics of wire mesh are yet to be determined. Experiments to date strongly suggest that the available guidelines for the design of wire

mesh will have to be modified by including the effect of the above parameters. In response to this need, the effect of various parameters is evaluated in the present research, and the results are used to modify the engineering equations presently available for the design of wire mesh as a bearing damper material.

Literature Review

Though wire mesh has been commercially available for a long time, there has been some limited research on its application as a bearing damper material, as follows.

Childs [4] reported tests conducted on wire mesh for possible use in the space shuttle main engines high-pressure fuel turbopump. The bench tests conducted on wire mesh showed "good" damping characteristics, but numerical quantities were not reported. A computer rotordynamic model, with the wire mesh damper installed in the supports was said to have much better performance than any other alternative available. Rivin [5] described the usage of wire mesh as vibration isolators. Barnes [6] used the wire mesh for aircraft engine mounts and suggested that the density of the wire mesh influence the stiffness to great extent. He also noted that the damping characteristics of the wire mesh are dependent on the material used.

Wire mesh was used by Okayasu et al. [7], for the first time as a bearing damper in a liquid hydrogen turbopump used in the LE-7 engine. The turbopump when used without the wire mesh faced several vibration problems. The use of wire mesh “friction dampers” in the bearing supports of the turbopump enabled the machine to operate at 46,139 rpm, which was higher than its third critical speed. They reported that wire mesh showed the most effective source of damping compared to the other damping components.

Wang Xin and Zhu [1] reported experiments that showed the wire mesh damper controlling three times more imbalance than the squeeze film damper.

Zarzour [3] tested wire mesh as bearing damper in a rotordynamic test stand for a turboprop engine rotor and his results indicated promising characteristics of wire mesh from the damping and stiffness point of view. The wire mesh damper, made of stainless

steel strands, was used to replace the squeeze film damper in the full-scale power turbine test rig. Unlike the SFD, the damping of the wire mesh did not show any significant change with temperature over the range 129°F - 210°F. Wire mesh was also tested soaked in oil to determine its behavior in practical applications and was found to work the same as when dry. The effect of radial interference on the rotordynamic characteristics of wire mesh was also reported.

Burshid [8] researched a hybrid damper seal design in which copper wire mesh was used for auxiliary sealing. The copper mesh was found to have more damping than stainless steel mesh.

Al-Khateeb and Vance [9] reported that the wire mesh dampers in parallel with a squirrel cage allow wider control of the support stiffness. Ertas, Al-Khateeb and Vance [10] showed that the wire mesh works even at cryogenic temperatures. Al-Khateeb [2] reported that the wire mesh bearing damper has characteristics comparable to those of the squeeze film dampers. Endurance tests on these dampers done over a period of six months showed little to no change in the damping characteristics. He reports that the dynamic characteristics are dependent on the radial strain amplitude and axial strain (compression). He also suggests that the effect of axial thickness of the mesh have to be investigated.

TEST METHODOLOGY

Non-rotating dynamic tests were conducted on different wire mesh elements to analyze the effect of axial thickness, radial thickness, axial compression, radial interference, and displacement amplitude. The results from these tests were used to update the design guidelines for wire mesh as a bearing damper. Tests were also conducted to study the effect of a wire mesh with radial splits and a mesh comprised of two radial segments.

Darlow [11] explained a detailed procedure for the design of elastomers. A similar approach was used for designing wire mesh dampers. These tests were conducted along the same guidelines keeping in mind the main objective of forming a design procedure for wire mesh dampers. A simple product solution (1) was assumed and the parameters were varied one at a time. This insured that one particular group of test analyzed the effect of change in just one parameter.

$$K, C, H \propto fn(AT).\ fn(RT).\ fn(AC).\ fn(RI).\ fn(Amp) \qquad (1)$$

This product solution is utilized in forming the design guidelines for wire mesh as a bearing damper.

Using the test rig described in the next chapter, the wire mesh was subjected to periodic chirp vibration excitations through a 0-200Hz-frequency range. The vibratory displacement and the shaker force data were collected using a two-channel signal analyzer. The results were averaged over four excitation cycles. Using the sensitivity of the proximity probe (197.5 mils/V) and the force transducer (0.04402 V/lb.) this data was analyzed using a MathCAD worksheet, which is included in Appendix C.

Parameter Identification

The following data were recorded and stored for each excitation set:

- Linear Magnitude of transfer function (X/F)

- Phase angle of the transfer function (X/F)
- Coherence
- Real part of the transfer function
- Imaginary part of the transfer function
- Linear magnitude of Displacement Amplitude (X)
- Linear magnitude of Force Amplitude (F)

The test rig was modeled over the frequency range of interest as a single degree of freedom system and was represented by the following second order non-homogeneous linear differential equation with constant coefficients:

$$M\ \ddot{x}(t) + K\ \dot{x}(t) + C\ x(t) = f(t) \quad \text{.....(2)}$$

Considering a harmonic steady state solution as $x = Xe^{i\omega t}$ and $f(t) = Fe^{i\omega t}$ where X and F are complex entities the frequency response function is given by:

$$F / X = (K - M\omega^2) + iCw \quad \text{.....(3)}$$

$$\mathrm{Re}(F / X) = K - M\omega^2 \quad \text{.....(4)}$$

$$\mathrm{Im}(F / X) = C\omega \quad \text{.....(5)}$$

The magnitude and phase of the complex number are given by (6) and (7)

$$\|F / X\| = \sqrt{\left(K - M\omega^2\right)^2 + \left(C\omega\right)^2} \quad \text{.....(6)}$$

$$\phi = \tan^{-1}\left(\frac{C\omega}{K - M\omega^2}\right) \quad \text{.....(7)}$$

The real part of the transfer function is a parabola and represents stiffness when $\omega = 0$. This method of curve fitting the real part of F/X to obtain the stiffness coefficient is reasonable for a linear system and acceptable for weakly non-linear systems.

By collecting the dynamic Stiffness frequency domain data for a SDOF system having the wire mesh damping element, the stiffness and damping coefficients can be extracted by curve fitting the collected data to the above equations. Several curve-fitting techniques were used depending on the type of data and the parameter to be extracted.

Using data for the amplitude of dynamic stiffness, a polynomial curve fit was used to determine the values of K, M and C. However, more accurate estimates of damping were obtained when the amplitude of flexibility (inverse of dynamic stiffness) is used, i.e., when X/F data is used instead of F/X. This is due to the fact that minimal values of F/X occur in the region surrounding the natural frequency (around peak displacement amplitude). This is where the effect of damping is most evident. However, the small F/X values make curve-fitting schemes, such as the method of least squares, insensitive to errors in that region. Hence, damping values estimated from that region of F/X may not be accurate. On the other hand, the X/F values are highest in the vicinity of resonance. Therefore, a good approach for estimating damping from X/F data would be to analyze the data surrounding resonance.

After evaluation of several parameter identification schemes, two were selected for analyzing the FRF data. The presented values are averages of results obtained from these methods. They are discussed in more detail in the next sections. Appendix C shows the MathCAD® worksheet that was written for the parameter identification of a SDOF system using these methods for a viscous damping model.

90-Degree Phase Method

This is the classical 90-Degree phase method based on the fact that amplitude of a SDOF system's dynamic stiffness transfer function at resonance, is equal to the viscous damping coefficient (C) multiplied by its resonance (or natural) frequency (ω_n).

$$(\omega_n)^2 = K/M \quad (8)$$

when $\Omega = \omega_n$ (i.e., at resonance), the amplitude of dynamic stiffness transfer function is given by:

$$F/X|_{\Omega = \omega n} = C \cdot \omega_n \quad (9)$$

The system's natural frequency (ω_n) is determined from phase data when the phase angle is equal to 90 degrees. The viscous damping coefficient (C) can be calculated from the transfer function amplitude at that frequency using the above equation.

In the parameter identification MathCAD® worksheet (Appendix C), the phase data is analyzed using a routine developed to more correctly estimate the natural frequency by minimizing the error. The output frequency, and the K and M values are then utilized by another subroutine to determine the transfer function value at the natural frequency (through a linear fit of surrounding points) and calculate the viscous damping coefficient (C).

This method is particularly useful for analysis of SDOF systems (within the testing frequency range). The method is quite sensitive to initial guess values, which may require iterative modification to obtain more accurate results. Thus for each test data the guess value is varied till the most accurate value of 90 degree phase is obtained. This is especially required when the system has very low damping and the phase graph changes immediately.

Nonlinear Regression Method

This method utilizes an internal non-regression routine in MathCAD® that can be used for fitting a nonlinear function to a set of data points. The transfer function is represented by a nonlinear function that could be fitted through polynomial techniques (e.g. using the square of F/X amplitude data).

This nonlinear regression method uses a vector with elements consisting of the nonlinear function (model to be fitted) and its partial derivatives with respect to each parameter (K, M and C) to determine the least-squares parameter values that best fits the collected data within the specified analysis range (see Appendix C). The method requires some initial guess values for the parameters to be determined. This method is usually independent of the initial guess value and gives accurate results in almost all cases, but sometimes when the guess is too much off then it may require a second guess. The values of K, C, M determined from this method may sometime turn out to be negative.

Appendix C shows a MathCAD worksheet, which uses the curve fit method and the 90-degree phase method to obtain the stiffness and damping coefficients for the wire mesh bearing damper. The final values are obtained by taking the average of the two methods.

TEST HARDWARE, APPARATUS, AND INSTRUMENTATION

The tests were done on a non rotating test rig, which is shown in Figures 1 and 2. Figure 3 shows the schematic diagram of the test rig along with the instrumentation setup.

The test rig has a cantilever beam attached at its base. The outer end of the beam has a steel journal attached to it and is surrounded by a rigid hollow cylindrical casing. This casing is used to mount the wire mesh housing adapter and the proximity probe. A rectangular block of steel is attached at the top of the journal to serve as a convenient reference for the proximity probe and also for the application of shaker force. The housing adapters are secured to the casing using four bolts such that they have almost infinite stiffness, as compared to the mesh and hence do not play any major role in the vibration testing. Wire mesh is secured inside the housing adapter, and when required, is compressed using the compression ring from top. A PCB force transducer is attached to the stinger to measure the force transmitted by the shaker. The force transducer is installed towards the journal end of the stinger to avoid any errors in the measured force signal. Proximity probe and transducer signals are collected using the dual channel signal analyzer. Adjusting the gain in shaker amplifier unit, controls the magnitude of force applied. The test rig has its first natural frequency close to 76 Hz.

The journal was machined from time to time to fit in the inner diameter of the wire mesh. Several new aluminum housing adapters and compression rings were fabricated to enable the testing of wire mesh having different radial and axial thicknesses.

Figure 1 Non rotating test rig – Top View

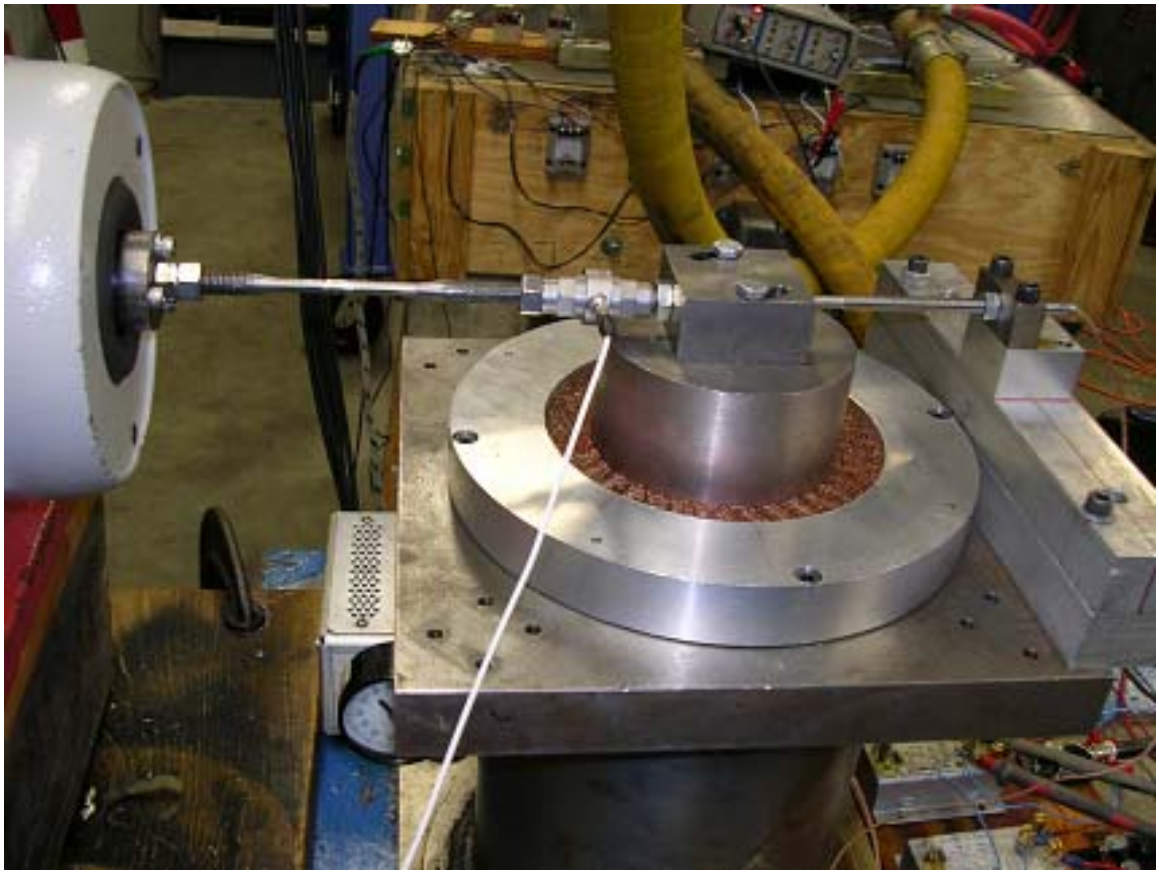

Figure 2 Non rotating test rig – Isometric view

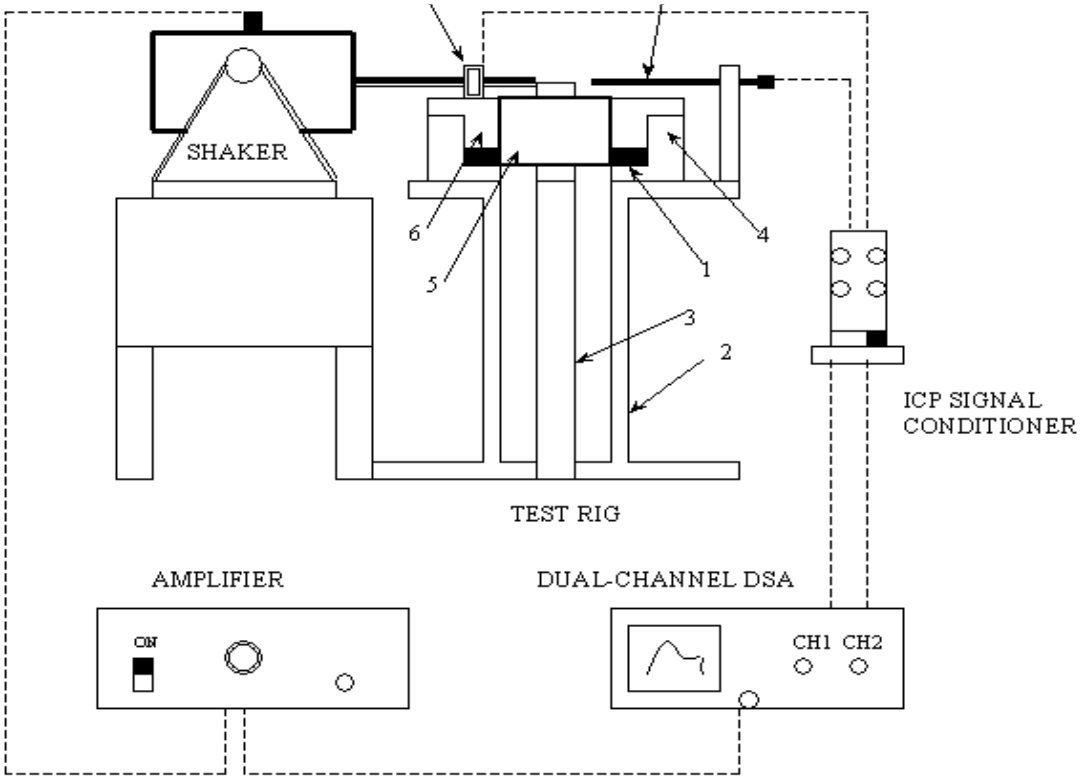

Item	Description
1	Wire mesh element
2	Test rig base/Casing
3	Shaft
4	Housing ring
5	Journal
6	Cover plate
7	Force transducer
8	Proximity probe

Figure 3 Schematic of the test rig along with the instrumentation set up

Wire Mesh Element Description

Seven groups of wire mesh elements (donuts), knitted with Jersey-Stitch were tested. The meshes were made of copper wire of diameter 0.0126" and were manufactured by "Metex Corporation". The specifications of the wire mesh tested along with their labels are shown in Table 1 and Figures 4, 5 and 6.

Table 1 Specification of the wire mesh tested and their labels

Group	ID (Inches (mm))	OD (Inches (mm))	Rad Thickness (Inches (mm))	Axial Thickness (Inches (mm))	Density (%)
A	4.019(102.08)	4.574(116.17)	0.277(7.035)	0.496(12.598)	36
O	4.007(101.77)	5.006(127.15)	0.499(12.674)	0.492(12.496)	42.5
N	3.939(100.05)	5.458(138.63)	0.759(19.278)	0.499(12.674)	42.7
B	4.007(101.77)	5.006(127.15)	0.499(12.674)	0.492(12.496)	42.5
M	3.939(101.05)	6.979(177.26)	1.519(38.582)	0.499(12.674)	42.7
P	3.939(101.05)	5.458(138.63)	0.759(19.278)	0.499(12.674)	42.7
S	3.939(101.05)	5.458(138.63)	0.759(19.278)	0.499(12.674)	42.7

The Group A element had a single radial slit in it and had much lower density as compared to the rest of the samples. Group M, P and S were made from meshes similar to that of group N. Group M was made by radially stacking mesh from group N and two split meshes of the same group such that it had twice the thickness of the mesh N. This left a small gap on both sides of the outer mesh. To ensure that this does not produce error in the results, mesh from group P (also split) was tested and compared against group N, which was a complete donut. The Group S element comprised of two segmented mesh parts, having a radial angle of 130 degrees each. Group B comprised of two identical split meshes similar to the O group, stacked one over the other axially to give twice the axial thickness of a single mesh.

The material density used in calculating the wire mesh element densities for commercial 99.9% copper wire is 0.295 lb/in^3 (8166kg/m^3). The wire mesh density is defined as follows:

$$\text{Wire Mesh Element Density} = \frac{\text{Weight of Wire Mesh Element}}{\text{Total Volume} \times \text{Wire Material Density}} \qquad (10)$$

This is the same as the volumetric density ratio calculated by dividing the volume of meshed wire by the total volume of the wire mesh element.

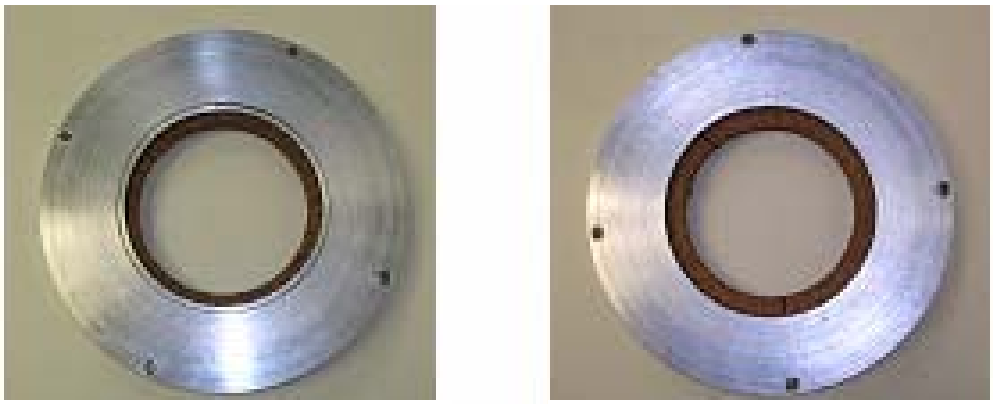

A **O**

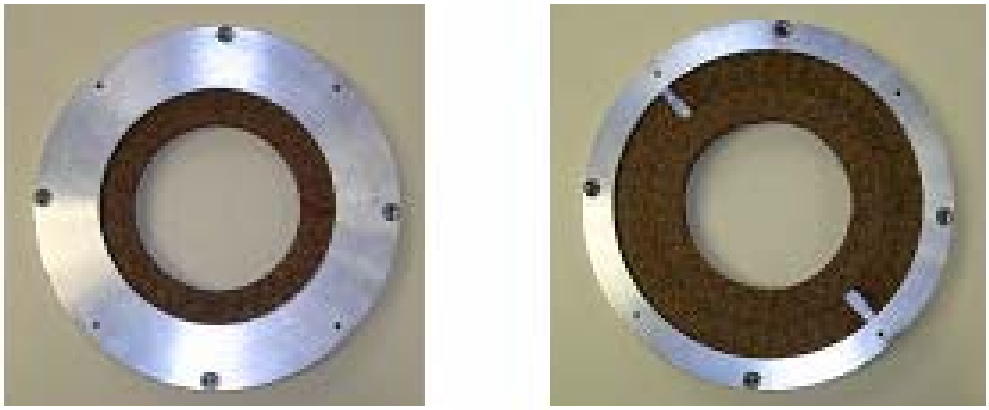

N **M**

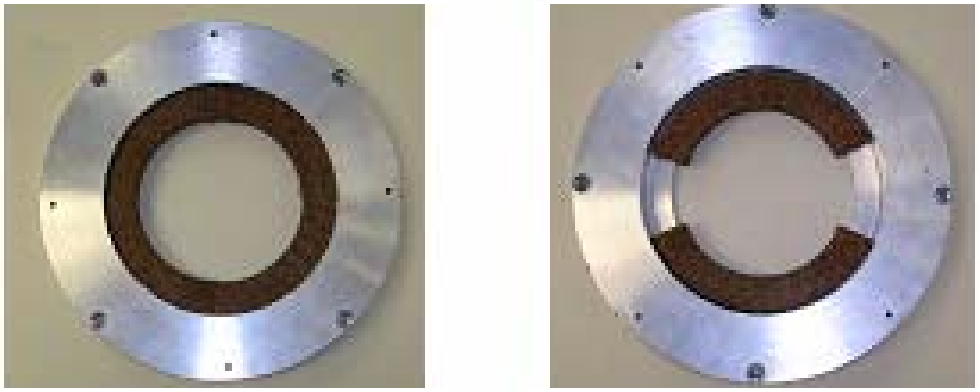

P **S**

Figure 4 Wire mesh elements

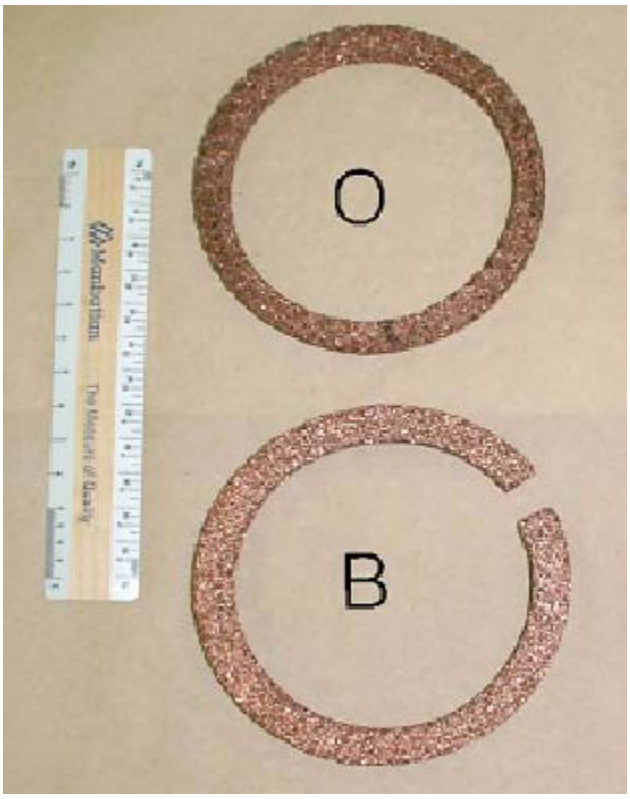

Figure 5 Wire mesh element O and B

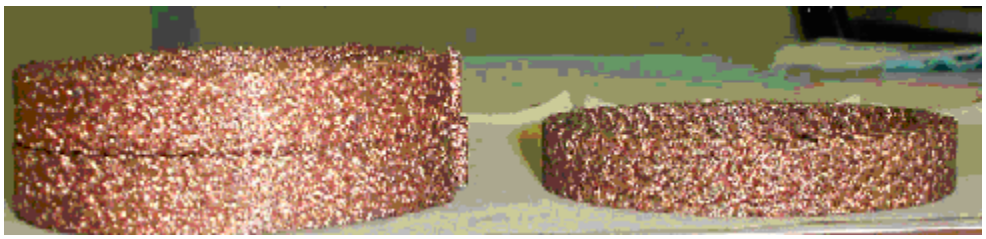

Figure 6 Wire mesh element B stacked

BASELINE MEASUREMENTS

In all, seven groups of experiments were performed. Shaker tests were conducted on the test rig with the necessary instrumentation as explained in Chapter V. Initial tests were performed to collect the baseline data (without the wire mesh installed in the housing) and baseline stiffness and damping coefficients were extracted. The MathCAD worksheet, Appendix C, was used to extract damping and stiffness coefficients from the measured data in the form of transfer functions, coherence and linear X and F plots. A total of four averages were taken for each configuration.

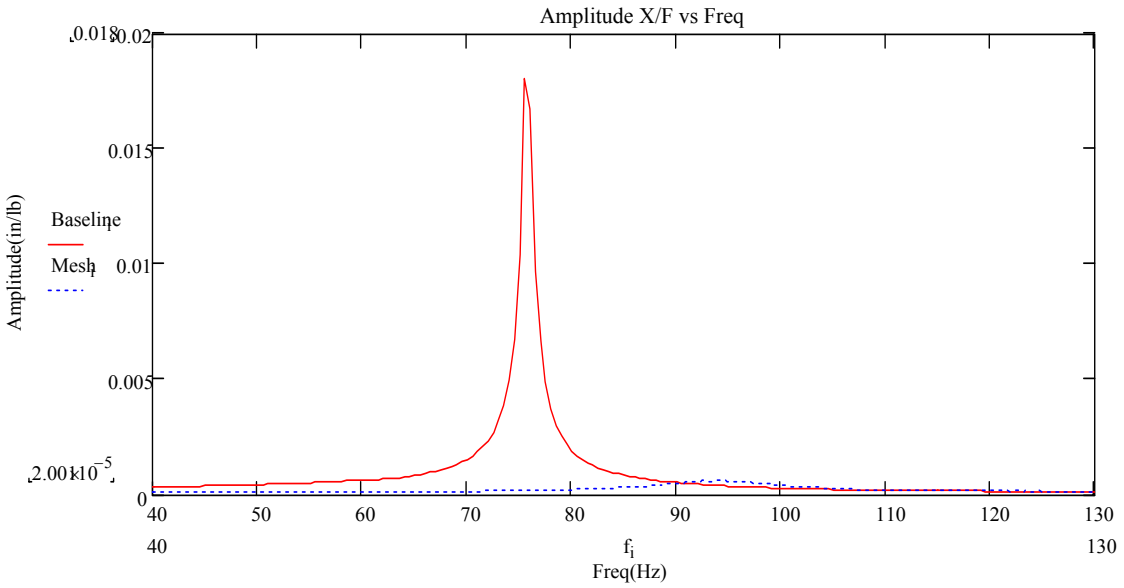

Figure 7 Typical X/F transfer function (magnitude) plot

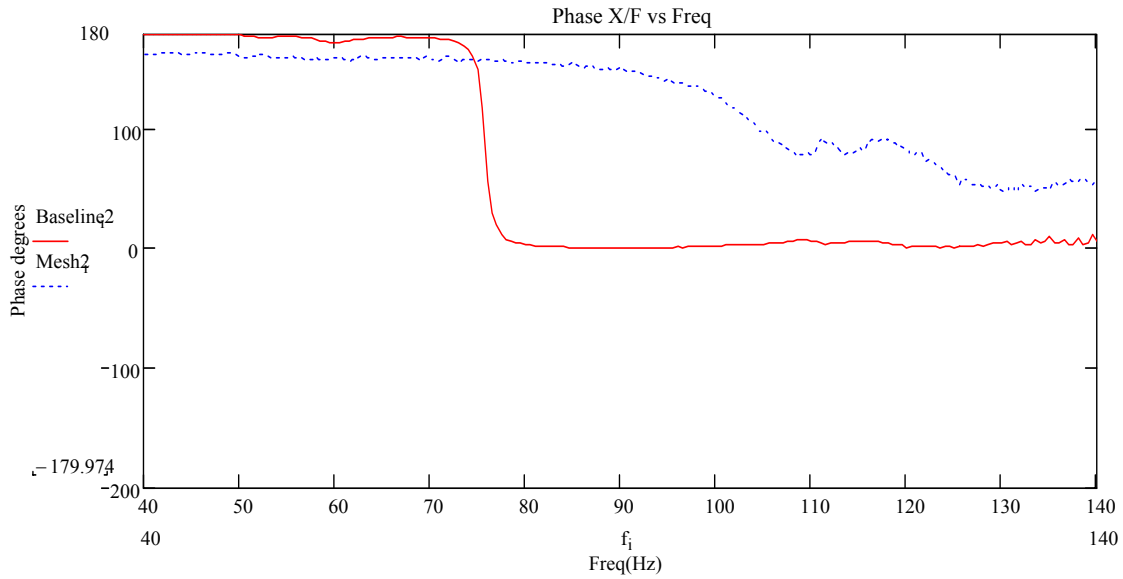

Figure 8 Typical transfer function phase(X/F) plot

Figures 7 and 8 show typical transfer function plots recorded by the signal analyzer. The plots show data collected for the test rig with and without the wire mesh donut installed. Referring to Figures 7 and 8, it can be observed that the wire mesh offers a lot of positive damping and moderate stiffness. From the X/F transfer function plot, it is seen that the amplitude at the critical is highly suppressed.

The gradual change in the phase plot and the clear comparison of the magnitude transfer function plots indicate significant damping from the wire mesh. The baseline coefficients were subtracted from the measured values to obtain the effective stiffness and damping coefficients. For this test rig, the baseline stiffness was found to be 3510.6 lb./in and the corresponding damping value was 0.141 lb.-sec/in without the wire mesh installed. The baseline test rig coefficients were subtracted from the equivalent system coefficients obtained from shaker tests with the wire mesh element installed. The resulting values were then multiplied by a factor to obtain the actual stiffness and damping coefficients (contribution to mass is negligible) of the wire mesh element. This multiplication factor is due to the pivoted nature of the journal's motion, and the fact that the displacement probes and the force transducer are not installed exactly at the wire

mesh location. The correction factor consists of two parts. First, the difference of elevation between the shaker/proximity probe location and where the wire mesh elements are installed in the test rig. The second reason is the difference of modal displacement at these two locations. Figure 9 shows the modal displacement of the test rig journal assembly as measured and calculated by Al-Khateeb [2].

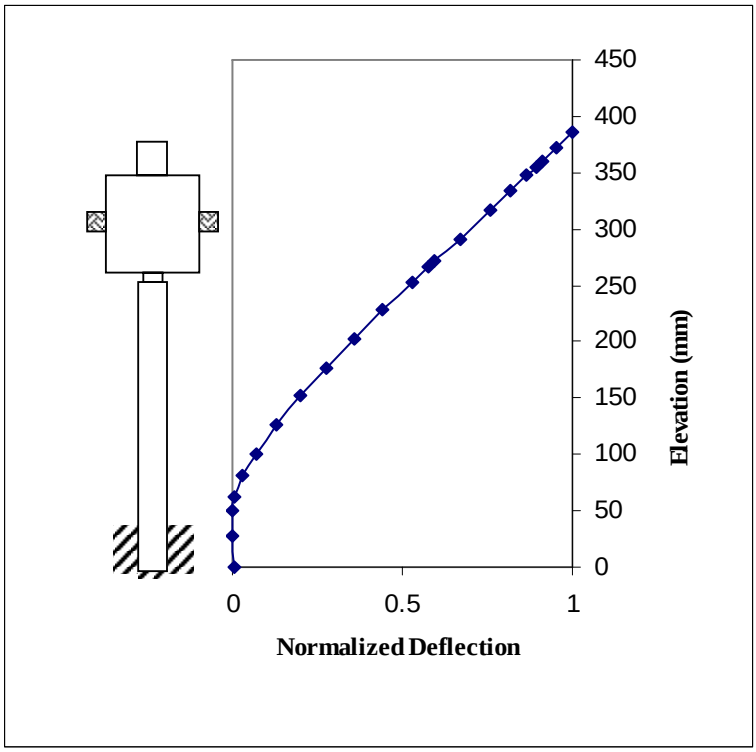

Figure 9 Calculated deflected shape of shaker test rig journal assembly

Having measured the different elevations and calculated the mode shape, the multiplication factor is calculated in the following manner:

Distance Ratio = Measurement Elevation / Wire Mesh Elevation

Deflection Ratio = Deflection at Measurement Level / Deflection at Wire Mesh Level

Multiplication Factor = Distance Ratio x Deflection Ratio

This factor was used in the MathCAD worksheet to obtain the true X/F data at the wire mesh location. This factor was modified for some tests because the deflection ratio was not same for all the meshes. The housing adapters used for the axial thickness testing were at a much higher level on the test rig than the ones used for the rest of the tests. This caused a variation in the deflection ratio.

EFFECT OF DESIGN FACTORS

Axial Thickness

Axial thickness is one of the major decisive factors in the design of wire mesh as a bearing damper. The testing with the O and B group samples were carried out to find a relation between the axial thickness and the rotordynamic coefficients. Both the groups were subjected to shaker tests. Two different approaches were used.

The initial idea was to emulate the results from testing of single wire mesh elements (‘O’ and ‘B’ group) obtained by Al-Khateeb [2] and then repeat the tests with two wire mesh elements stacked axially to give twice the axial thickness. The results from the previous testing could thus be used as a benchmark and would make things easier when it comes to comparison of results for thicker wire mesh elements. However, this turned out to be extremely difficult. Primarily, there was no record of the axial compression levels in the reports to imitate the test conditions and configuration that Al-Khateeb followed in his work. Also re-assembly of the test setup, use of different instruments and approach, introduced a considerable deviation in the testing. Hence it was decided to conduct entirely new tests for the B group, with controlled axial compression, both for single as well as double wire mesh elements. This would ensure that the basis for comparison of results from the two cases is logical and substantial.

In all the tests done for axial thickness variation, the radial strain was found by dividing the radial displacement by the radial thickness of wire mesh. The radial displacement was found by measuring the time trace of the proximity probe signal. This was different from the displacement measured in the rest of the tests done in this research, where the radial displacement was found from the linear magnitude of 'X', that is, the proximity probe signal. It is to be noted that the above two methods give values which differ by order of magnitude.

To study the effect of increase in the axial thickness of the wire mesh, damping and stiffness coefficients were extracted from the X/F data. The measured values for the ‘O’ group samples are shown in Table 2 for 2.4% axial compression level. The variation

of the damping and stiffness coefficients with radial strain is shown in Figures 10 and 11 respectively.

Table 2 Damping and stiffness coefficients for the 'O' group elements – 2.4% compression

Radial strain (ε)	Proximity probe signal (0-pk volts)	Damping (lb.-sec/in)		Stiffness (lb./in)	
		Single mesh	Double mesh	Single mesh	Double mesh
0.0016	0.137	6.256	8.830	6641.209	17176.237
0.0045	0.386	3.938	8.628	4421.041	11392.047
0.0098	0.841	2.263	4.690	3257.113	8179.797
0.0198	1.73	2.335	3.915	2471.439	4768.335

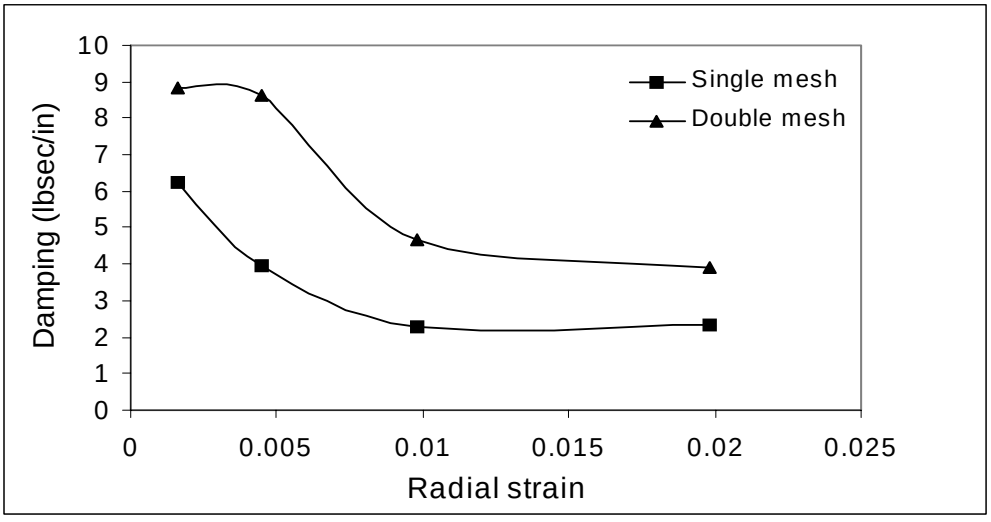

Figure 10 Variation of damping coefficients with radial strain for 'O' group elements for an axial compression of 2.4%

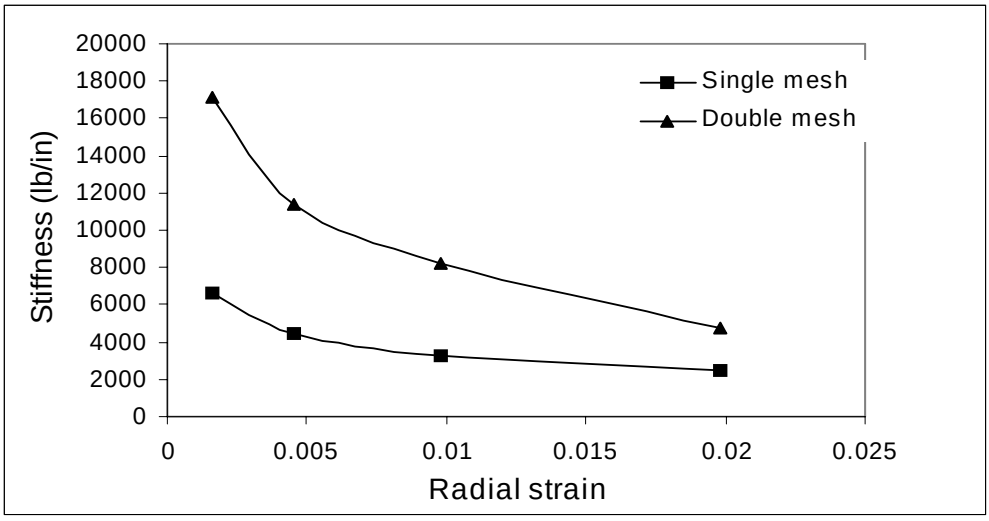

Figure 11 Variation of stiffness coefficients with radial strain for 'O' group elements for an axial compression of 2.4%

Keeping the primary objective of investigating the effect of axial thickness in mind, from above figure it can be infered that both the damping and stiffness coefficients are greater for thicker elements. However a closer look at the coefficients reveals that there is not a fixed relationship between the two parameters. Table 3 and Figure 12 higlight the percentage increase in damping and stiffness values for a two fold increase in the axial thickness of 'O' group elements.

Table 3 Percentage increase in damping and stiffness coefficients for the 'O' group elements

Radial strain	% Increase in damping	% Increase in stiffness
0.0016	41.1445	158.6312
0.0045	119.096	157.6779
0.0098	107.247	151.1364
0.0198	67.66595	92.9376

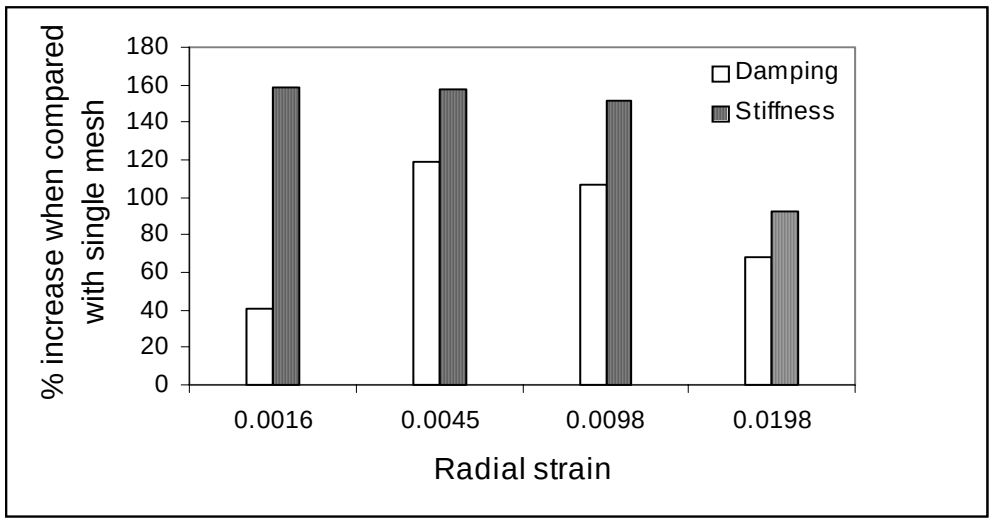

Figure 12 Percentage increase in damping and stiffness coefficients for the 'O' group elements for a two fold increase in axial thickness

These results only emphasize the trend of the coefficients with the increase in axial thickness but do not determine a quantitative relationship. The testing with the 'B' group samples was thus carried out with a slightly modified procedure, aniticipating that the results would give a much better idea of the relation between the axial thickness and the coefficients. The modified procedure is described as follows: The single mesh element 'B' was tested using the same procedure followed for the 'O' group elements. Axial Compression levels of 0%, 1.25, 2.5% were applied and for each compression level, the mesh was subjected to maximum radial strains of 0.00473, 0.00947, 0.01421, 0.01895. These uniformly stepped values of axial compression levels and radial strain were chosen to have a more direct comparison between each case. For testing the double mesh, two 'B' group elements were stacked and the compression ring was hand tightened and the coefficients were extracted immediately. Following the assumption of liniear variation of coefficients with axial thickness, the coefficients would be doubled for a wire mesh twice as thick. If this was not the case, then the hand tightness was varied to match it. Further tests were done with this compression as reference.

The following Table 4 shows the coefficients measured from the 'B' group samples for 0% and 2.5% axial compression levels. The single mesh values are those

obtained from testing with 'B' and for the double mesh configuration two 'B' elements were stacked one on the other.

Table 4 Damping and stiffness coefficients for 'B' group elements

0 % axial compression								
Radial strain	Damping				Stiffness			
	Single mesh		Double mesh		Single mesh		Double mesh	
	lb.-sec/in	N-sec/m	lb.-sec/in	N-sec/m	lb./in	N/m	lb./in	N/m
0.00473	1.84	322.00	3.68	644.00	1002.16	175378	2091.71	366049
0.00947	1.11	194.25	2.13	372.75	929.50	162662	1711.08	299439
0.01421	0.75	131.25	1.64	287.00	889.66	155690	1680.81	294141
0.01895	0.65	113.75	1.36	238.00	581.95	101841	1239.63	216935
2.5 % axial compression								
Radial strain	Damping				Stiffness			
	Single mesh		Double mesh		Single mesh		Double mesh	
	lb.-sec/in	N-sec/m	lb.-sec/in	N-sec/m	lb./in	N/m	lb./in	N/m
0.00473	2.55	446.25	4.89	855.75	1338.14	234174	2619.89	458480
0.00947	1.58	276.50	3.49	610.75	1017.99	178148	2185.81	382516
0.01421	1.26	220.50	2.68	469.00	982.06	171860	2004.93	350862
0.01895	1.01	176.75	2.21	386.75	859.42	150398	1777.64	311087

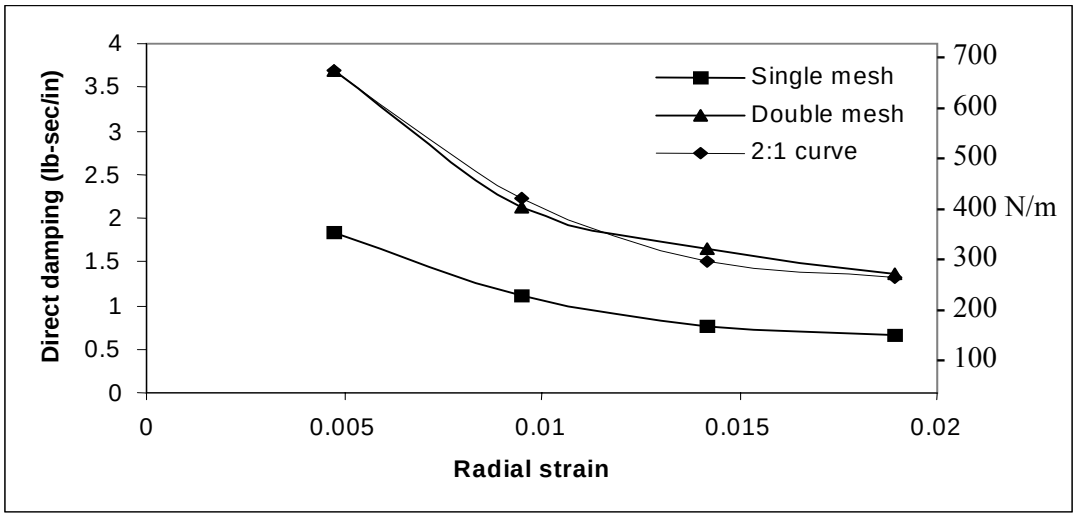

Figure 13 Variation of damping coefficients with radial strain for 'B' group elements for an axial compression of 0 %

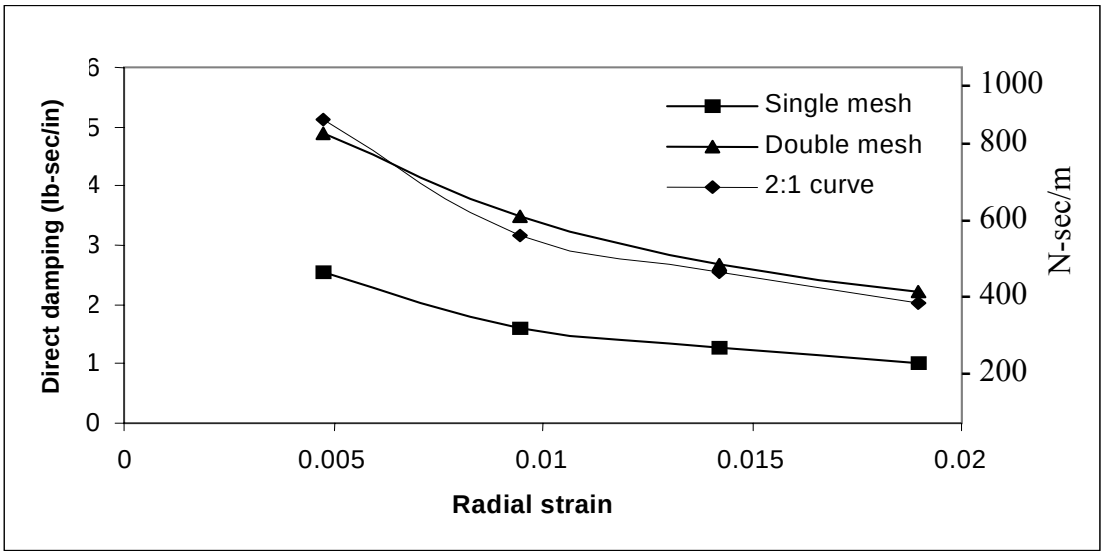

Figure 14 Variation of damping coefficients with radial strain for 'B' group elements for an axial compression of 2.5 %

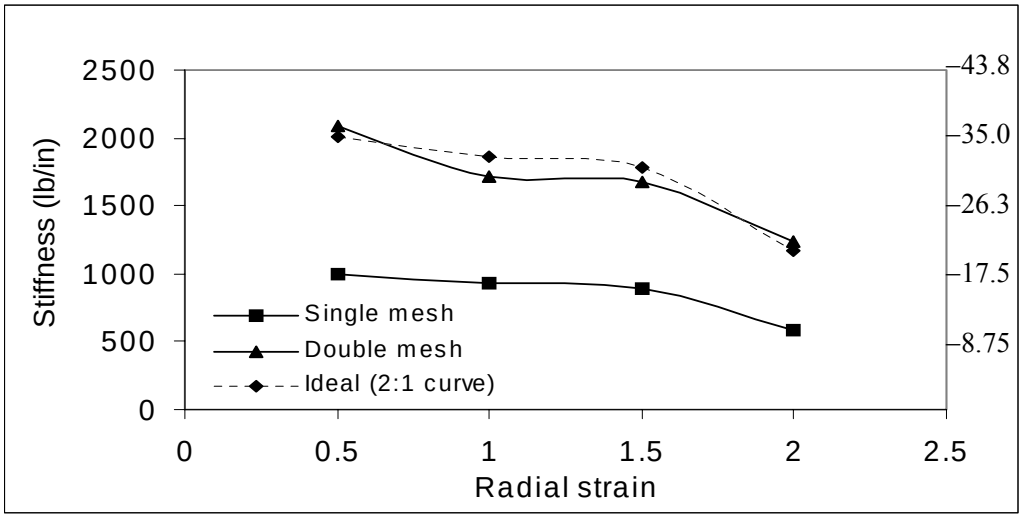

Figure 15 Variation of stiffness coefficients with radial strain for 'B' group elements for an axial compression of 0 %

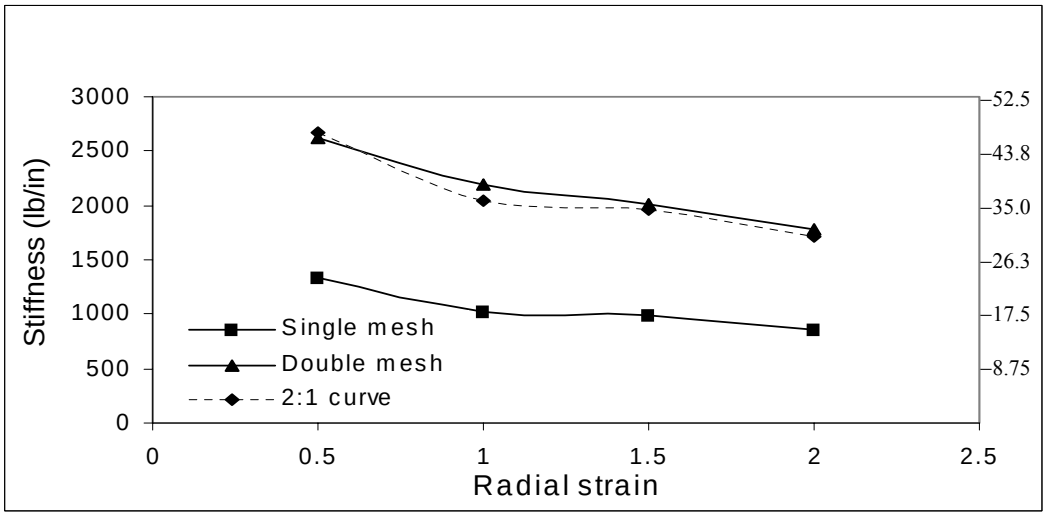

Figure 16 Variation of stiffness coefficients with radial strain for 'B' group elements for an axial compression of 2.5 %

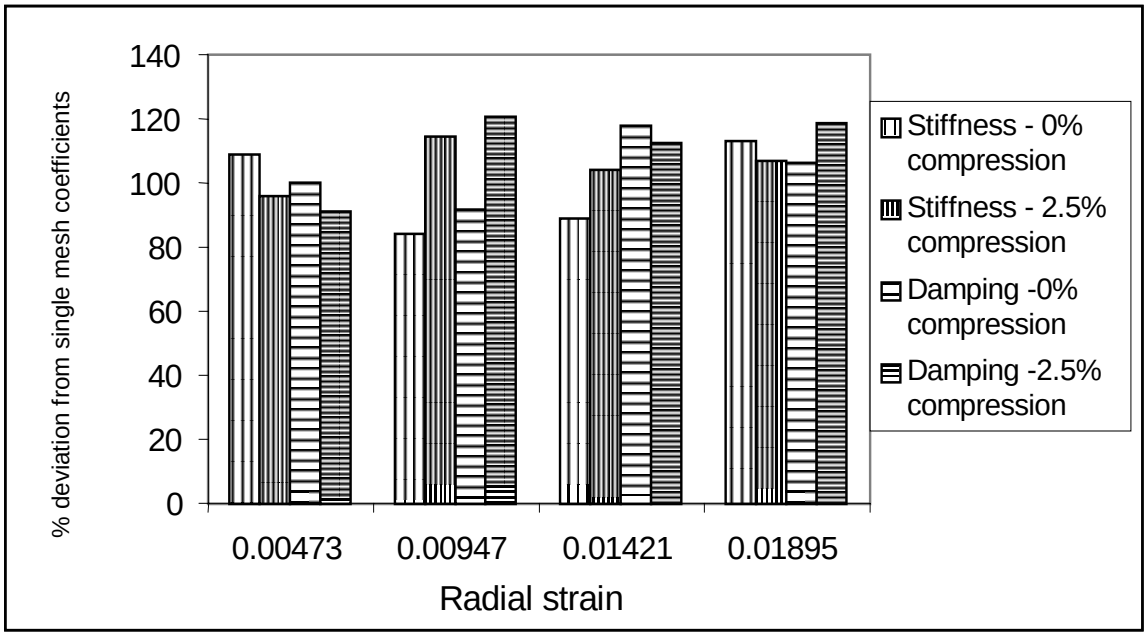

Figure 17 Percentage increase in damping and stiffness coefficients for the 'B' group elements for a two fold increase in axial thickness.

Figures 13 through 17 clearly demonstrate that both stiffness and damping coefficients increase by the same percentage as the axial thickness. In other words, the coefficients are linearly dependent on the axial thickness of the wire mesh. The 2 : 1 curve shown in all the plots refers to an ideal situation in which the stiffness and damping coefficients are exactly doubled for a two fold increase in the axial thickness of the wire mesh. These results agree very well with the formula solved by Zarzour [3].

Some deviation is observed from the ideal situation especially for the 2.5% axial compression level. This can be attributed towards unsymmetry in the boundary of the two wire mesh elements. It might be possible to realise the ideal case (2 : 1) if the thicker wire mesh elements were made of a single piece rather than two individual entities.

Radial Thickness

The objective of this section is to study the effect of variation in radial thickness on the stiffness and damping of wire mesh bearing damper. For the donut shape, which was used in these experiments, the radial thickness is defined as half the difference between inner and outer diameters. This is a primary design factor for the wire mesh donut as well as the hardware surrounding it. The results were used to form design equations for the dynamic coefficients of wire mesh bearing dampers.

Four sets of copper mesh donuts having different radial thicknesses were tested. The displacement amplitude, radial interference, axial compression and axial thickness were maintained constant so that the tests indicate only the effect of change in radial thickness. The meshes tested were from group A, O, N, and M. Mesh A was observed to have very high damping and to enable meaningful collection of data, it was decided to test with higher displacement amplitudes. This was decided by the maximum amount of force the shaker could exert. In this section all the tests were done with constant 0.5 mils displacement amplitude. Elements of group O, N, M were of nearly same density whereas element A was of much lesser density.

Figures 18 and 19 show the X/F transfer function magnitude and phase for different radial thicknesses. It can be easily deduced that stiffness and damping of the wire mesh damper decreases with increase in its radial thickness. Damping and stiffness coefficients were extracted using MathCAD and are shown in Table 5. From Table 5 it is seen that both stiffness and damping vary inversely with radial thickness. Figure 20 shows an almost linear relationship between stiffness and a radial thickness parameter (Ro+Ri)/(Ro-Ri) for the first three values of the data. The fourth value is for group A mesh, which is of much lower density than the other three. This may be the reason for its stiffness being much lower than what the curve fit shows. Thus comparing this value with the curve fit can also give a relation for density variation. This variation of stiffness and damping coefficients with the radial thickness parameter (Ro+Ri)/(Ro-Ri) agrees well with the formula solved by Zarzour [3] and the Beam column theory discussed by Darlow [11]. Similarly for damping it is seen from Figure 21 that it follows an almost

linear relationship. The relations below are utilized in the formulation of design equations.

$$K := Const \cdot \frac{Ro + Ri}{Ro - Ri} \qquad C := Const \cdot \frac{Ro + Ri}{Ro - Ri}$$

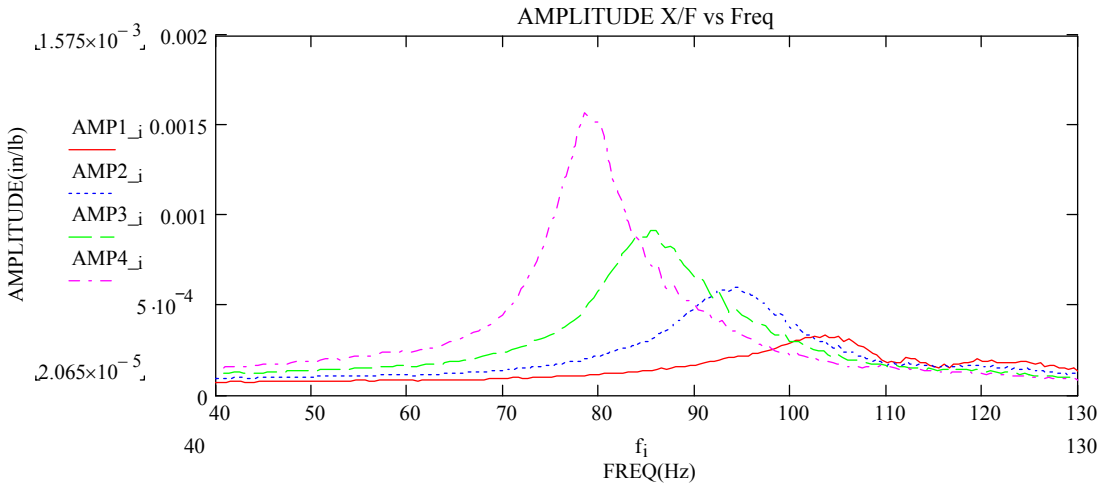

Figure 18 X/F Magnitude having radial thickness 1<2<3<4

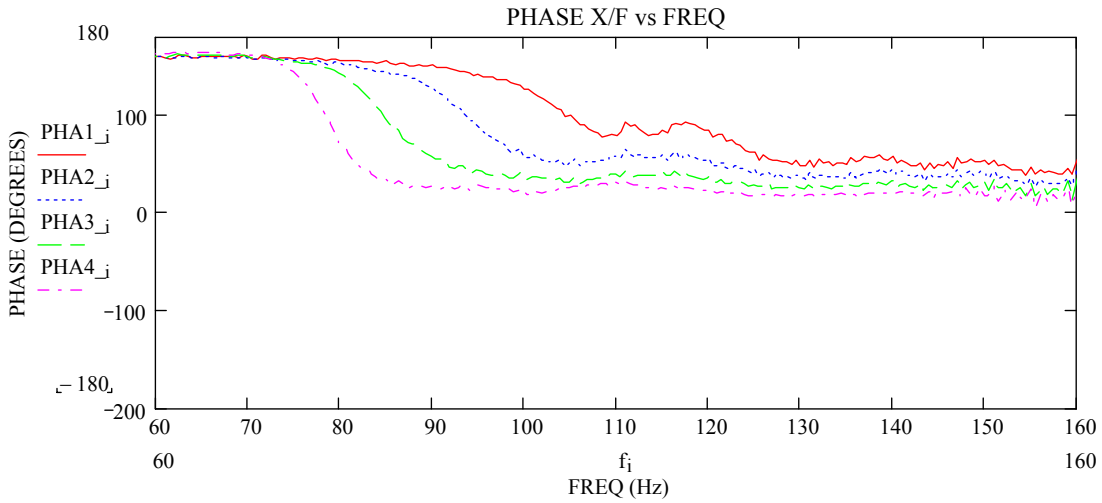

Figure 19 X/F phase having radial thickness 1<2<3<4

Table 5 Variation of stiffness and damping with radial thickness

Sr. No.	Rad. Thick (Ro-Ri)		Stiffness K		Damping C	
	in	mm	lb./in	N/m	lb.-sec/in	N-sec/m
1	0.277	25.40	1.45E+04	2.54E+06	4.951	866.43
2	0.499	50.80	1.21E+04	2.12E+06	2.763	483.53
3	0.759	76.20	7.79E+03	1.36E+06	1.9	332.50
4	1.519	101.60	4.82E+03	8.44E+05	1.1375	199.06

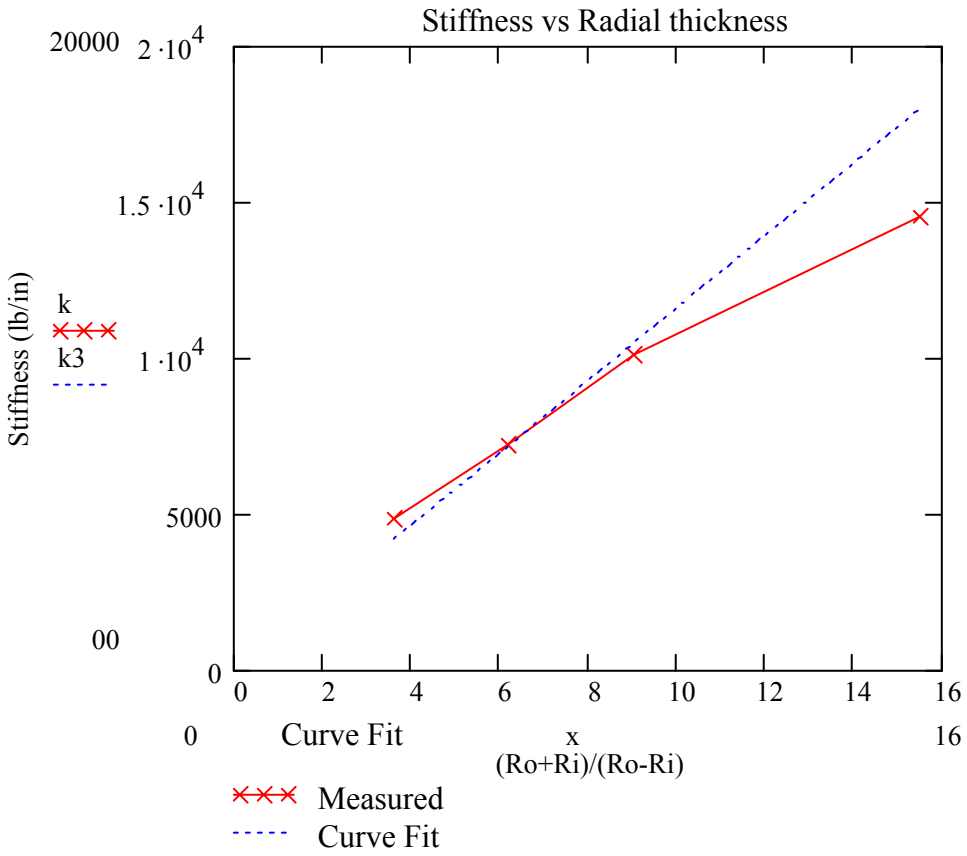

Figure 20 Variation of stiffness with radial thickness parameter

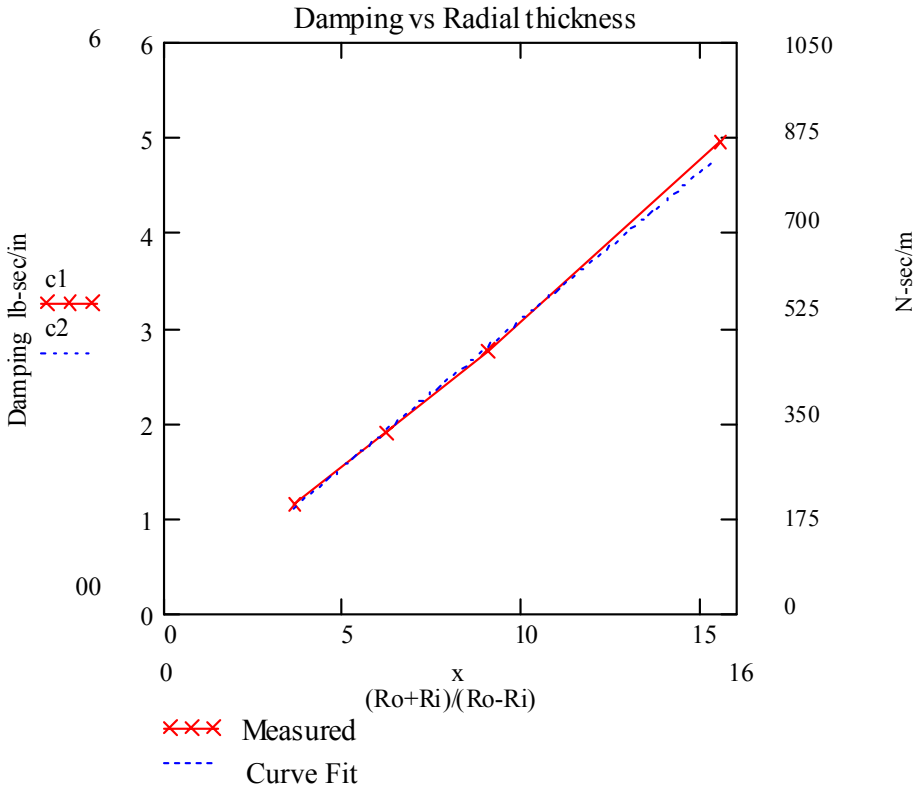

Figure 21 Variation of damping with radial thickness parameter

EFFECT OF INSTALLATION AND OPERATIONAL FACTORS

Axial Compression

The objective of this section is to investigate and quantify the effect of axial compression on the stiffness and damping of wire mesh when used as a bearing damper. The axial compression was applied to the thickness dimension of the donut shaped wire mesh element.

Group M was subjected to different levels of axial compression. As only one group of wire mesh elements was tested, the radial thickness and axial thickness were constant. Radial Interference was not applied in any tests and the displacement amplitude was maintained at 0.5 mils. The bolts in the compression ring were tightened to obtain various levels of axial compression. The gap between the housing adapter and the compression ring was measured using feeler gauges as shown in Figure 22. As the wire mesh surface is not completely even it is difficult to judge where the zero compression occurs, when the ring is installed. The procedure for measuring axial compression was different from that used in the previous sections. Zero axial compression was tested with no ring installed. The second test was done by hand tightening the bolts on the ring and considering that as the reference. All the measurements for the gap were made from this reference point. Later the data was curve fitted to find out the value of this reference. It was assumed that the amount of axial compression at reference is x mils so that the tests conducted are for 0, x, x+5, x+10, ...x+50 mils. The value of x is determined later from the curve fit. A total number of twelve different axial compression levels were applied.

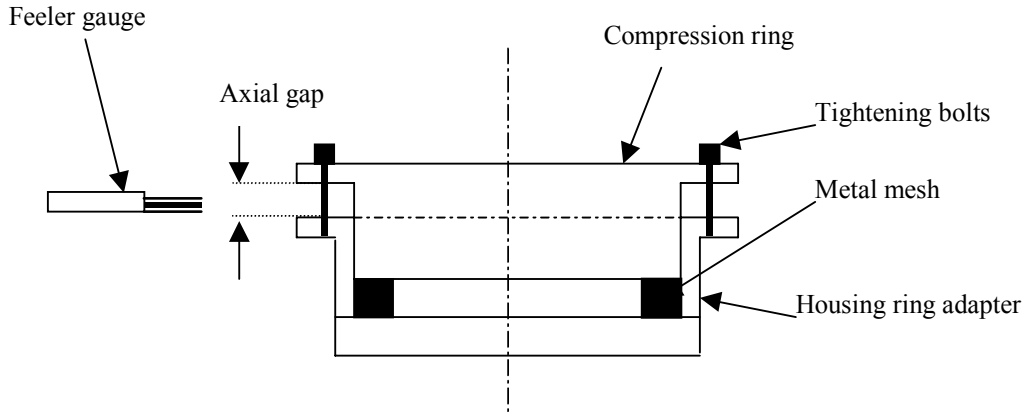

Figure 22 Application of axial compression

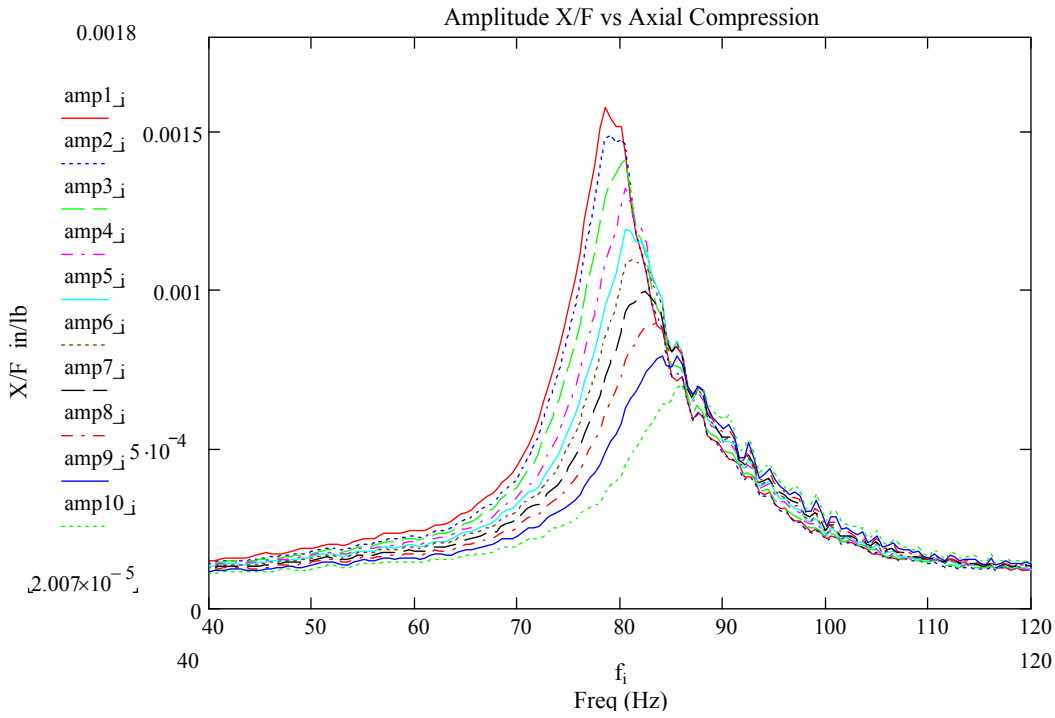

Figure 23 X/F Magnitude having axial compression 1<2<3.... <10

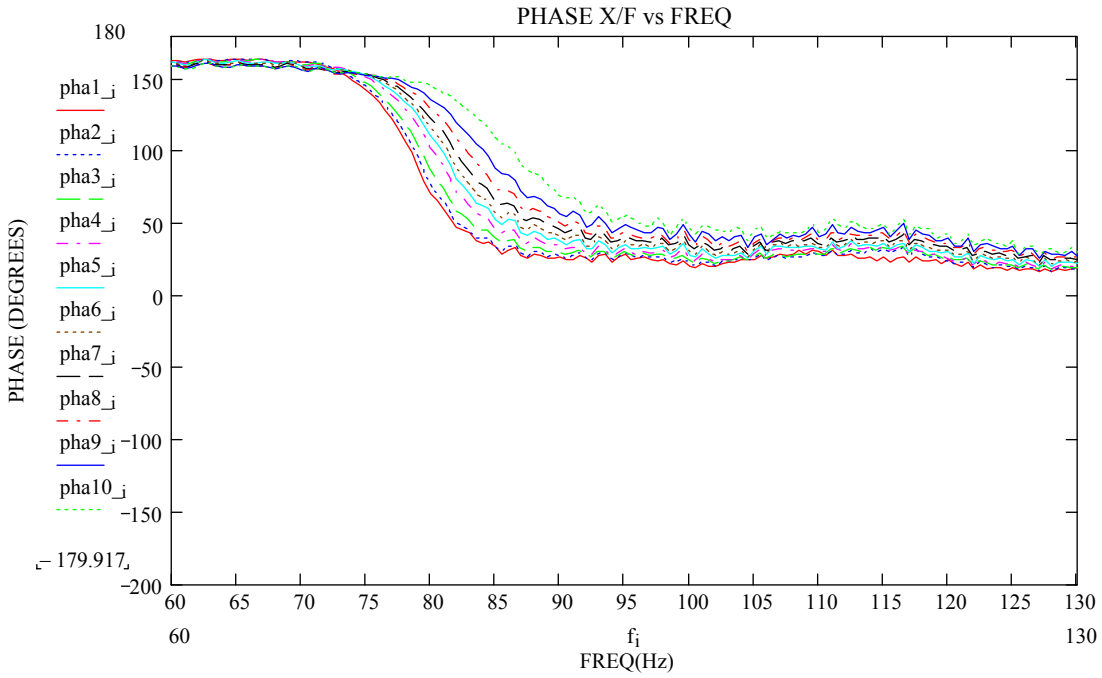

Figure 24 X/F Phase having axial compression 1<2<3.... <10

Table 6 Variation of stiffness and damping with axial compression

Sr. No.	Axial Compression		Stiffness K		Damping C	
	mils	mm	lb./in	N/m	lb.-sec/in	N-sec/m
free	0.00	0.00	4820.00	8.44E+05	1.14	199.06
Hand Tight(x)	15.00	0.38	5210.00	9.12E+05	1.18	206.33
x+5	20.00	0.51	5370.00	9.40E+05	1.28	223.91
x+10	25.00	0.64	5480.00	9.59E+05	1.30	226.80
x+15	30.00	0.76	5640.00	9.87E+05	1.39	243.25
x+20	35.00	0.89	5890.00	1.03E+06	1.51	263.99
x+25	40.00	1.02	6080.00	1.06E+06	1.64	287.79
x+30	45.00	1.14	6380.00	1.12E+06	1.79	313.86
x+35	50.00	1.27	6690.00	1.17E+06	1.98	346.59
x+40	55.00	1.40	7110.00	1.24E+06	2.22	389.20
x+45	60.00	1.52	7800.00	1.37E+06	2.49	436.36
x+50	65.00	1.65	8490.00	1.49E+06	2.70	472.41

Transfer function plots shown in Figures 23 and 24, respectively, indicate that the stiffness and damping coefficients for the wire mesh damper increase with the increase in axial compression. Further the extracted coefficients listed in Table 6 and plotted in Figures 25 and 26 strengthen this deduction. The data was curve fitted with a two-degree polynomial. By extrapolating the curve fit, the axial compression for the reference (hand tight) case was found out to be 15 mils, and the curves were redrawn with the actual values of the axial compression. This two-degree polynomial was used for quantifying the effect of axial compression on the design of wire mesh.

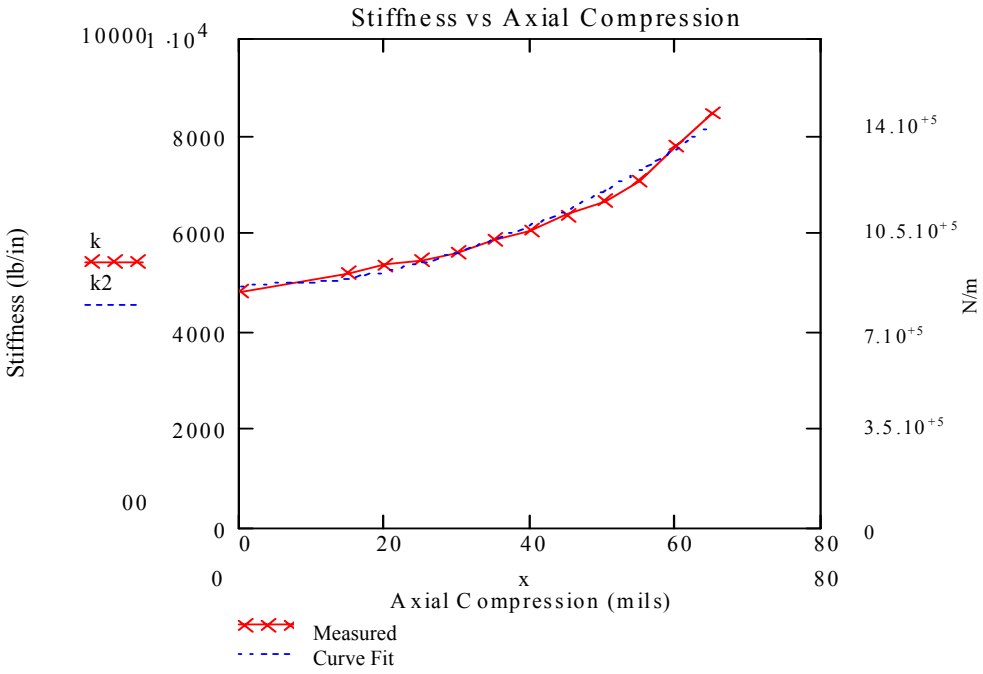

Figure 25 Variation of Stiffness with Axial Compression

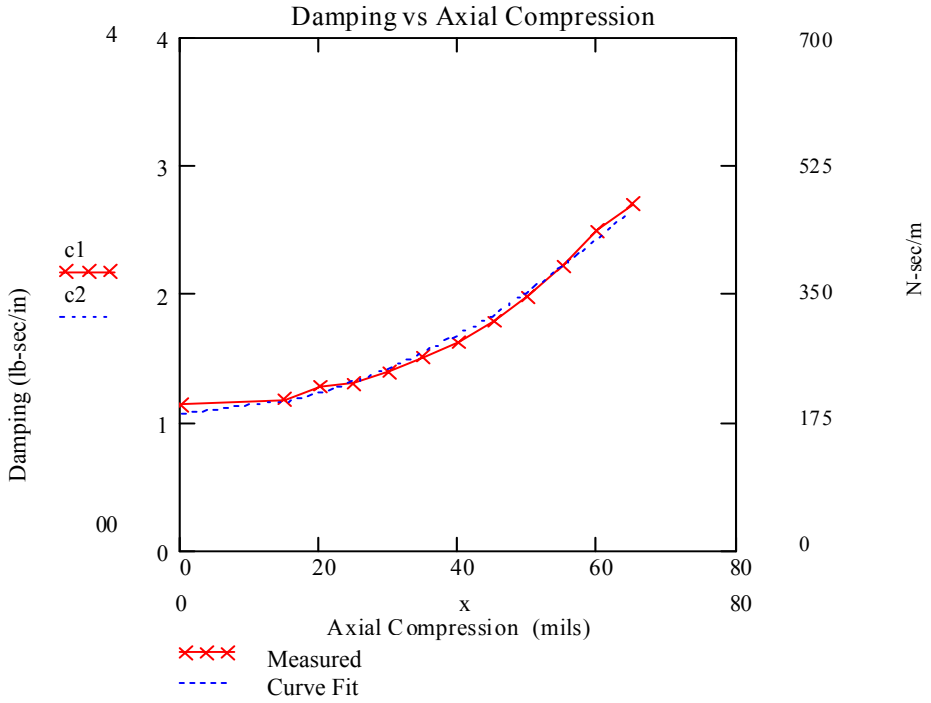

Figure 26 Variation of damping with axial compression

Radial Interference

The interference in the radial direction between the wire mesh damping element and its housing is an important design factor. The objective of this section is to quantify the effect of variation of radial thickness on stiffness and damping of the wire mesh bearing damper.

Radial interference was applied to the group M element while keeping all the other parameters constant. The displacement amplitude level was maintained at 0.5 mils throughout. The inner diameter of the housing adapters was varied to apply compression in the radial direction. To ensure a small variation in the radial interference and to increase the number of data points, aluminum tape of varying thickness was applied to the inside diameter of the housing adapter. The aluminum tapes used were very thin and had negligible damping.

The transfer function plots in Figures 27 and 28 indicate an increase in stiffness and damping with increase in radial interference. The extracted coefficients are plotted against the radial interference. Stiffness increases with increase in radial interference as can be seen from Table 7 and Figures 29 and 30. The data for stiffness in Figure 29 is fitted with a simple linear relation. With the exception of the first and the last data point the damping also exhibits a linear relationship with radial interference. These relations are used in the design equations explained at the end.

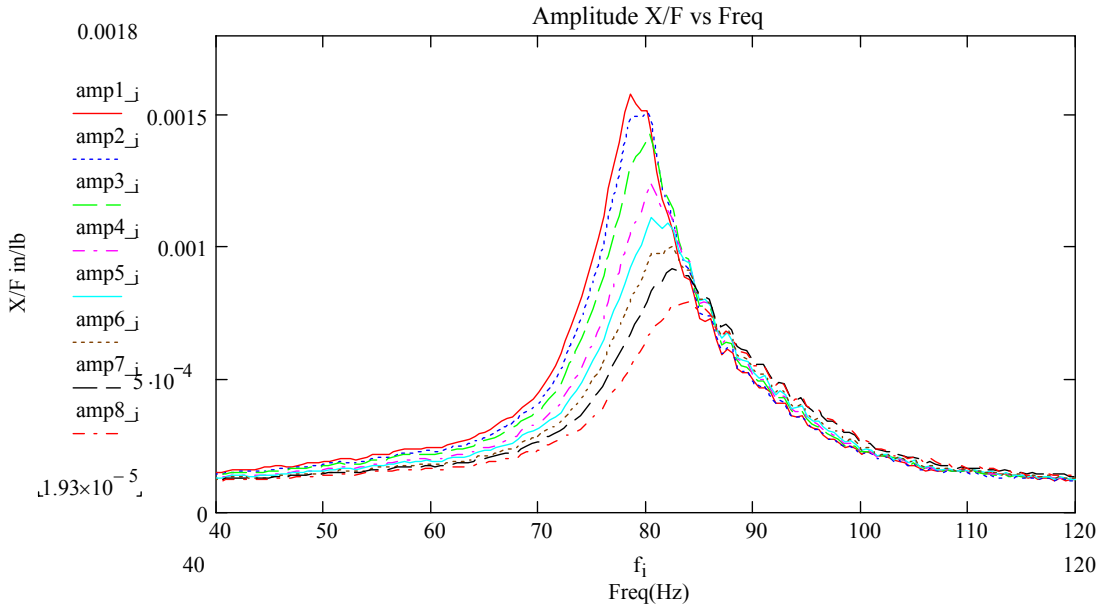

Figure 27 X/F Magnitude having radial interference 1<2<3.... <10

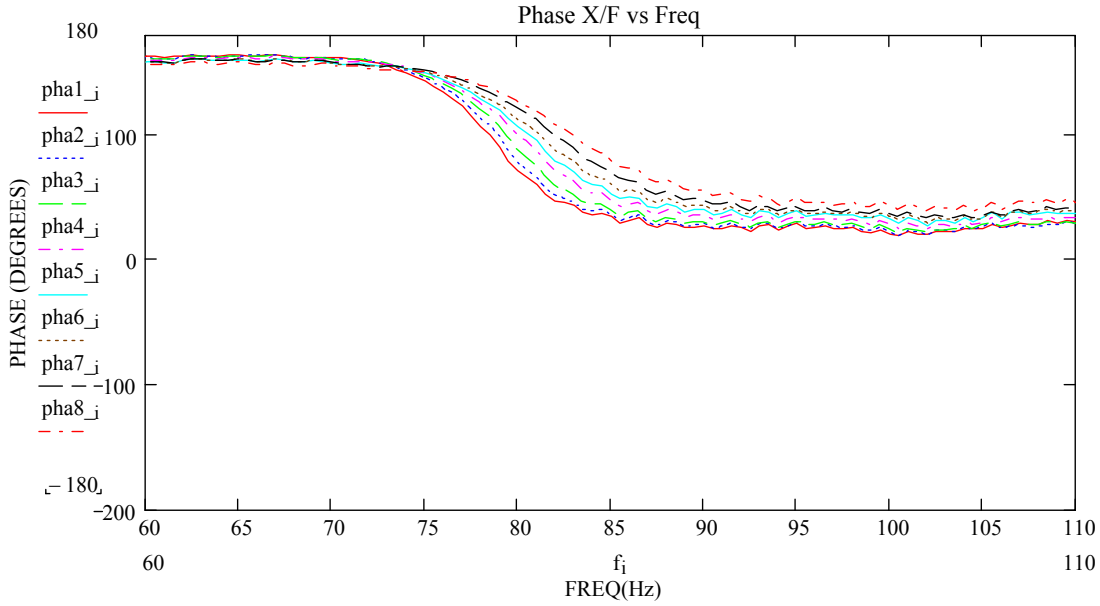

Figure 28 X/F Phase having radial interference 1<2<3.... <10

Table 7 Variation of stiffness and damping with radial interference

Sr. No.	Radial Interference		Stiffness K		Damping C	
	mils	mm	lb./in	N/m	lb.-sec/in	N-sec/m
1	0.00	0.00	4830	8.45E+05	1.1375	199.06
2	3.00	0.08	5110	8.94E+05	1.1640	203.70
3	6.00	0.15	5390	9.43E+05	1.2690	222.08
4	9.00	0.23	5670	9.92E+05	1.4340	250.95
5	12.00	0.30	5960	1.04E+06	1.6070	281.23
6	15.00	0.38	6240	1.09E+06	1.7695	309.66
7	18.00	0.46	6520	1.14E+06	1.9475	340.81
8	21.00	0.53	6800	1.19E+06	2.1995	384.91

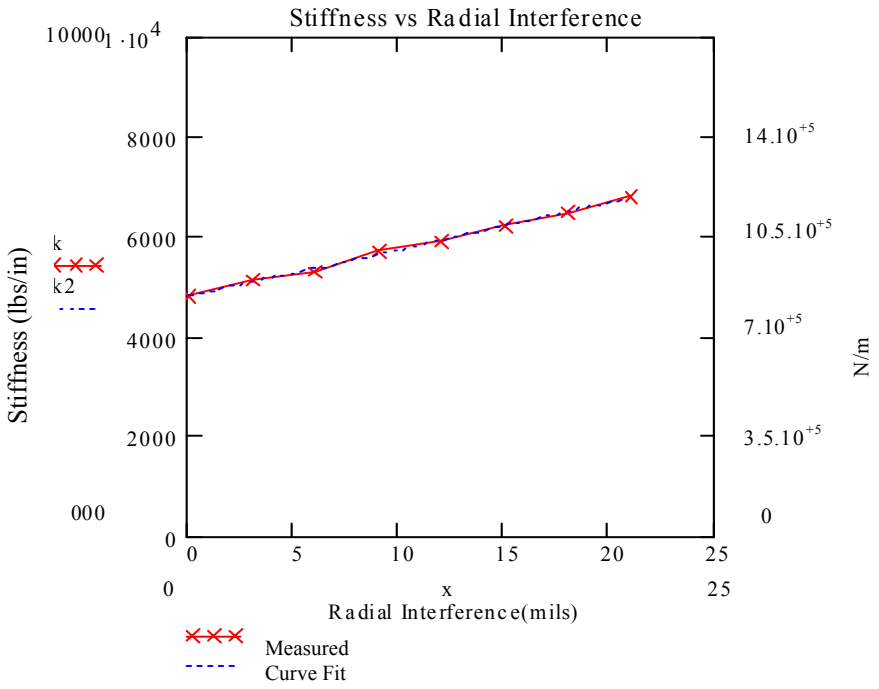

Figure 29 Variation of stiffness with radial interference

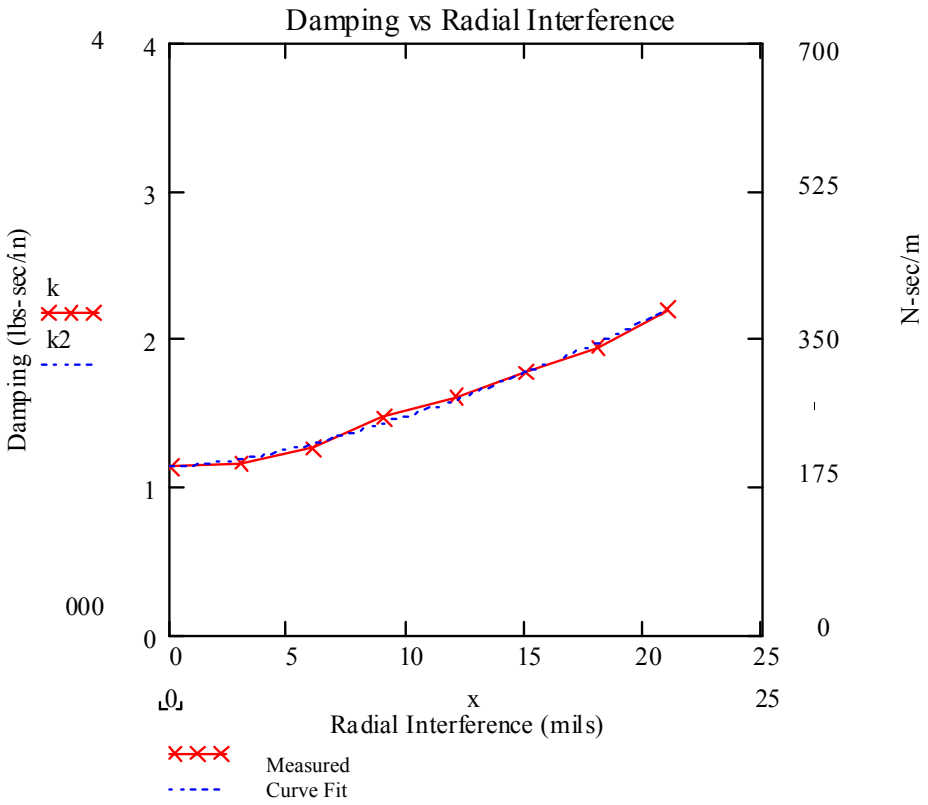

Figure 30 Variation of damping with radial interference

Displacement Amplitude

The stiffness and damping coefficients of the wire mesh are dependent on the variation of displacement amplitude and frequency to a large extent. Al-Khateeb [2], in his research, showed that the stiffness and damping vary inversely with the dynamic strain. The objective of this research was to obtain variation of the rotordynamic parameters of the wire mesh bearing damper with change in displacement amplitude.

Displacement amplitude was varied for group M element by varying the gain in the shaker amplification unit. All the other parameters were maintained constant. The maximum displacement amplitude was limited by the maximum force that the shaker could exert. Also at higher amplitudes of shaker force the data was blurred due to lot of

noise. Thus it was decided, to stay within a definite range of the displacement amplitude. Seven different values of displacement amplitude were tested.

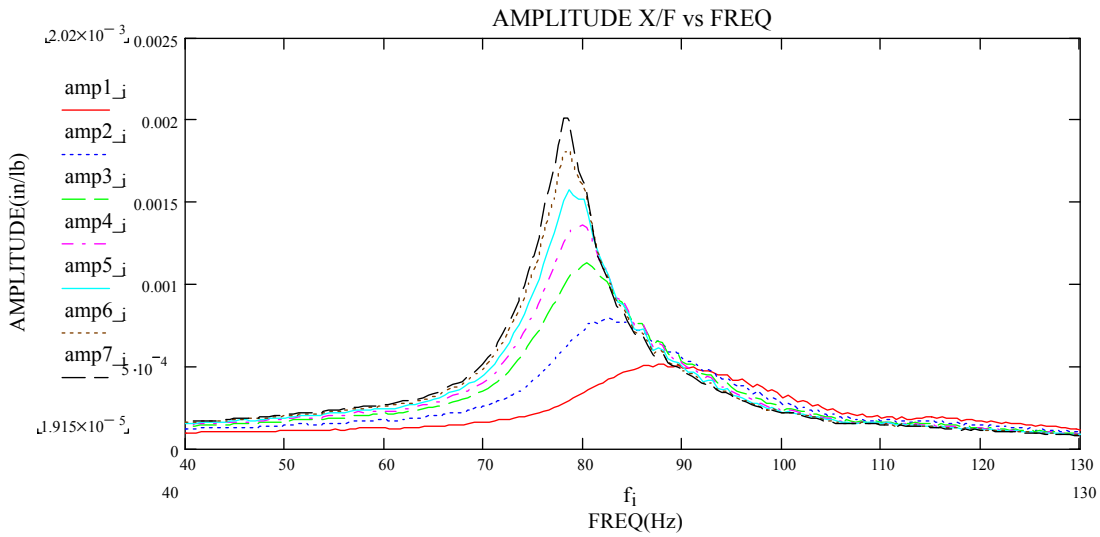

Figure 31 X/F Magnitude having displacement amplitude 1<2<3.... <10

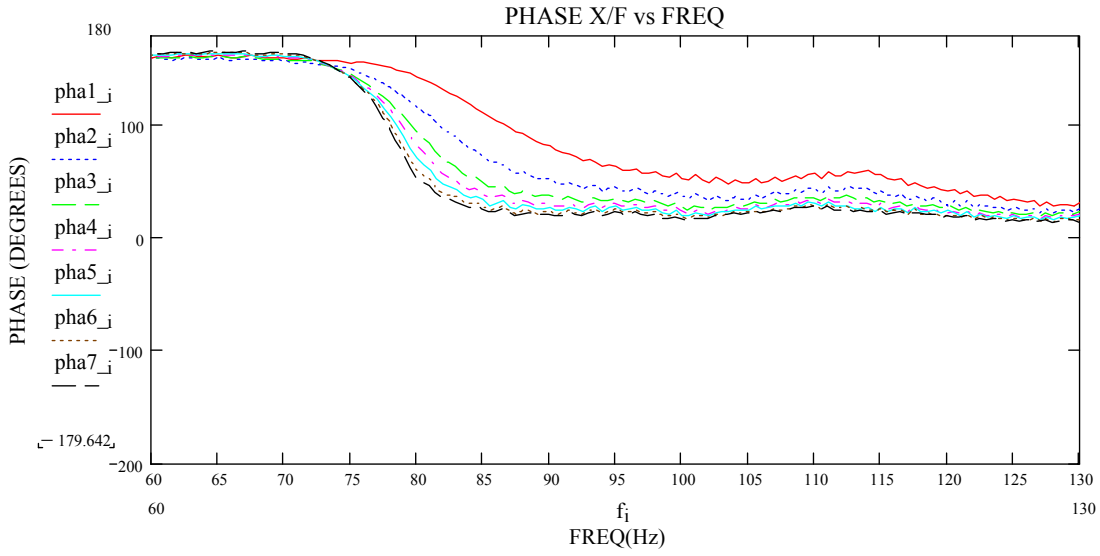

Figure 32 X/F Phase having displacement amplitude 1<2<3.... <10

Table 8 Variation of stiffness and damping with displacement amplitude

Sr. No.	Disp. Amplitude		Stiffness K		Damping K	
	mils	mm	lb./in	N/m	lb.-sec/in	N-sec/m
1	0.05	0.0013	8150	1.43E+06	3.2185	563.24
2	0.12	0.0030	6190	1.08E+06	2.2165	387.89
3	0.25	0.0064	5290	9.26E+05	1.5955	279.21
4	0.37	0.0094	4980	8.72E+05	1.3140	229.95
5	0.50	0.0127	4820	8.44E+05	1.1375	199.06
6	0.62	0.0157	4680	8.19E+05	0.9875	172.81
7	0.75	0.0191	4620	8.09E+05	0.8930	156.28

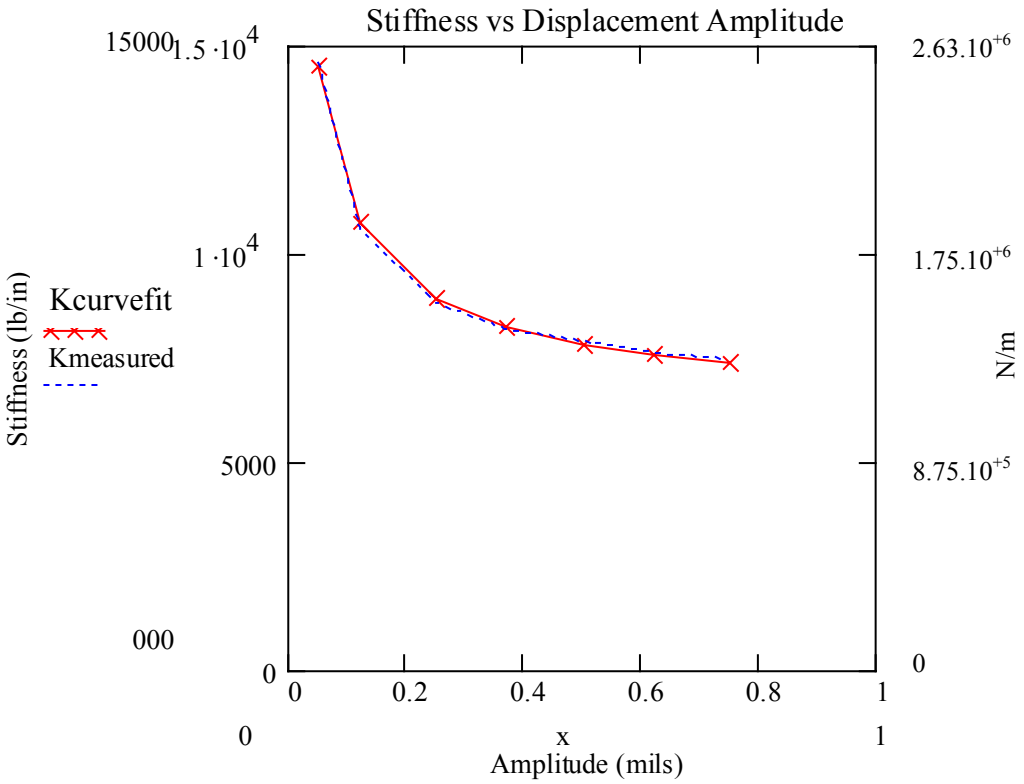

Figure 33 Variation of stiffness with amplitude

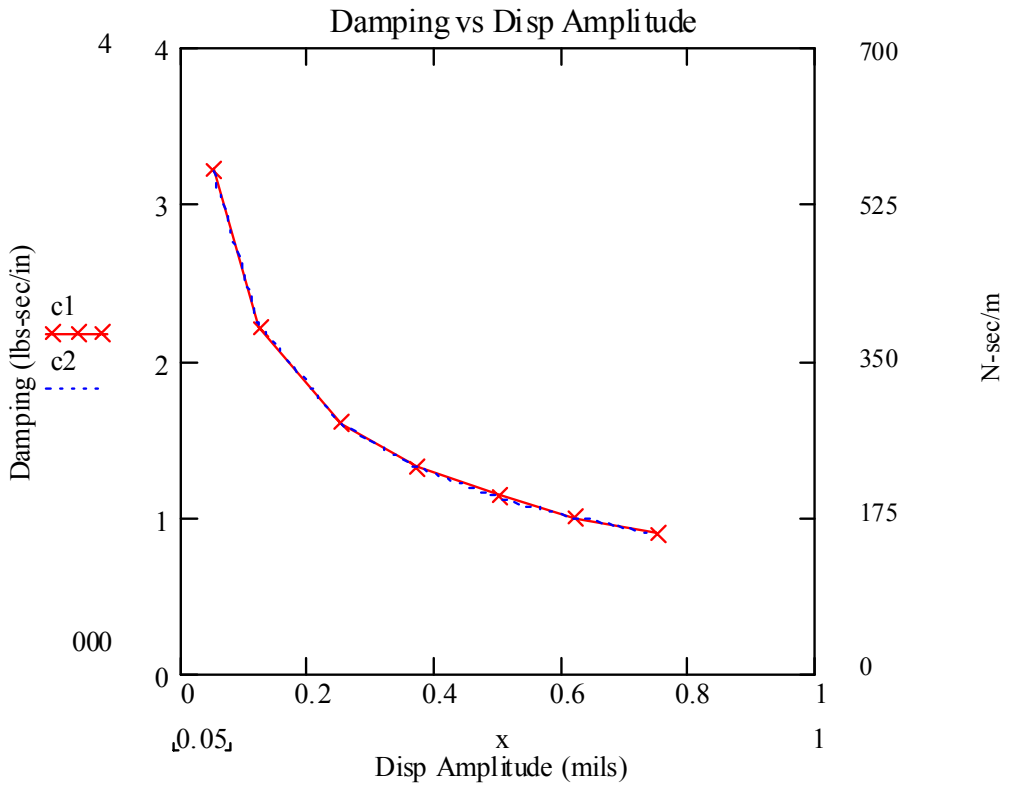

Figure 34 Variation of damping with amplitude

Transfer function plots in Figure 31 and 32 show that there is a significant decrease in damping as the amplitude is increased. The extracted coefficients are shown in Table 8 and plotted in Figure 33 and 34. Displacement amplitude has a considerable effect on the stiffness and damping of the wire mesh. Both the coefficients decrease as the amplitude increases. These findings are in agreement with the results of Al-Khateeb [2]. A polynomial of fourth degree was in close agreement with the data. Another fit that was considered was a linear relationship of $A^{-2/3}$, also in close agreement with Al-Khateeb's findings.

EFFECT OF ALTERNATIVE DESIGN

Split Mesh

Elements of group N and P were tested to study the effect of a split in the wire mesh donut. Al-Khateeb [2] in his research had already shown that the change of stiffness and damping with the orientation of split was not of significant importance. The present testing aims at comparing a split mesh with an unsplit (whole) mesh donut. The split was tested at an angle of 45 degrees from the shaker. Al-Khateeb had shown that the damping and stiffness of a split mesh are maximum at an angle of 45 degrees.

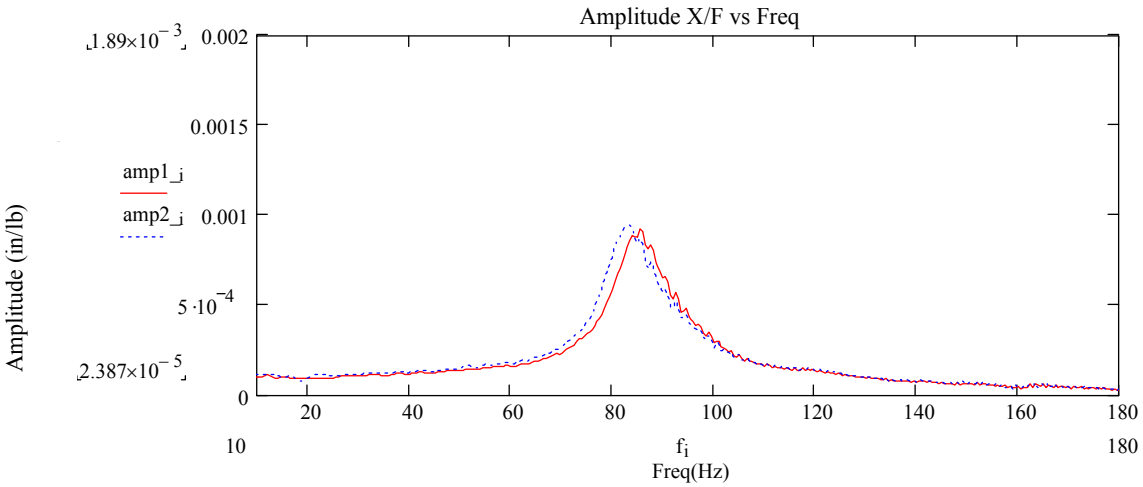

1-whole 2-split

Figure 35 Effect of radial split on transfer function magnitude

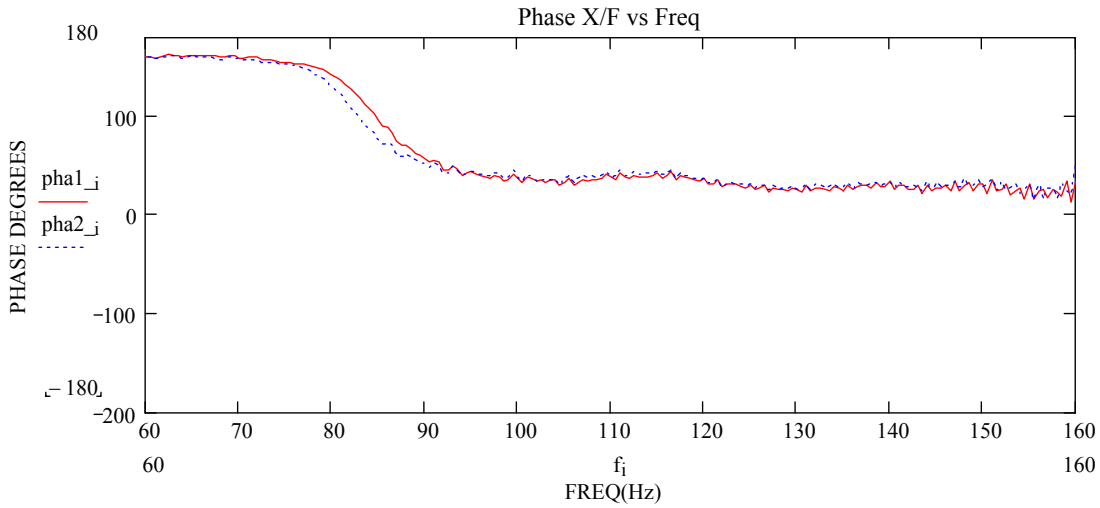

1-whole 2-split

Figure 36 Effect of radial split on transfer function phase

Table 9 Effect of radial split on the wire mesh coefficients

Sr. No.	Stiffness K		Damping C		%Change
	lb./in	N/m	lb.-sec/in	N-sec/m	
No Split (N)	4820	8.44E+05	1.1375	199.06	2.89
Split (P)	4670	8.17E+05	1.1162	195.34	1.58

The transfer function plots in Figures 35 and 36 indicate that there is only a small change in the coefficients when the split mesh is used. Table 9 shows that there is only a small percentage decrease in the value of stiffness and damping coefficients when there is a split in the mesh. This justifies the use of two split meshes while testing group M meshes.

Segmented Mesh

The segmented Mesh S is made up of two radial segments each having an arc of 130 degrees. These segments were tested in line with the shaker (vertical shaker force in Figure 4 Mesh 'S') and the results were compared against the tests of group N elements, which is a complete donut. The advantage of using this mesh is ease of installation and accommodation of small variations in the internal and external diameters of the wire mesh.

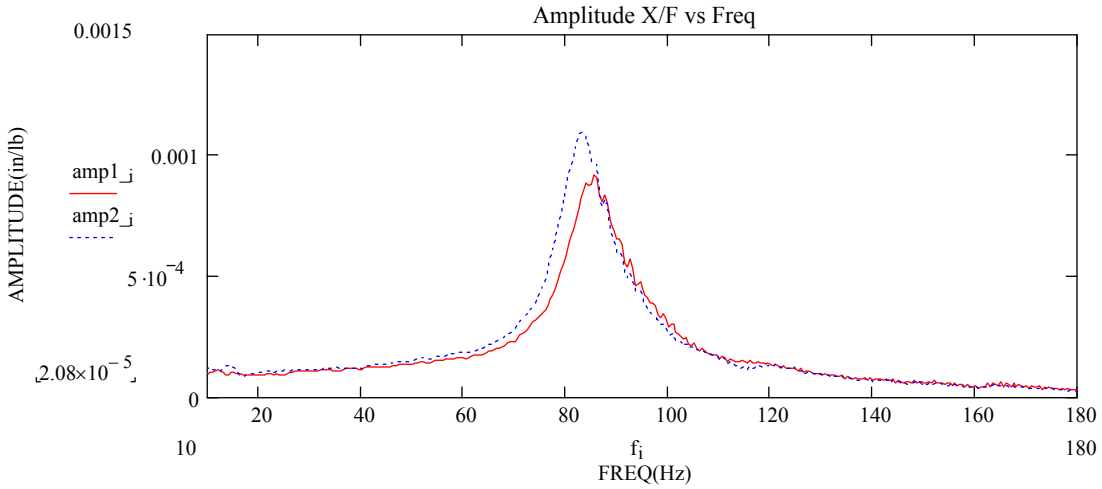

1-whole 2-segmented

Figure 37 Effect of radial segment on transfer function magnitude

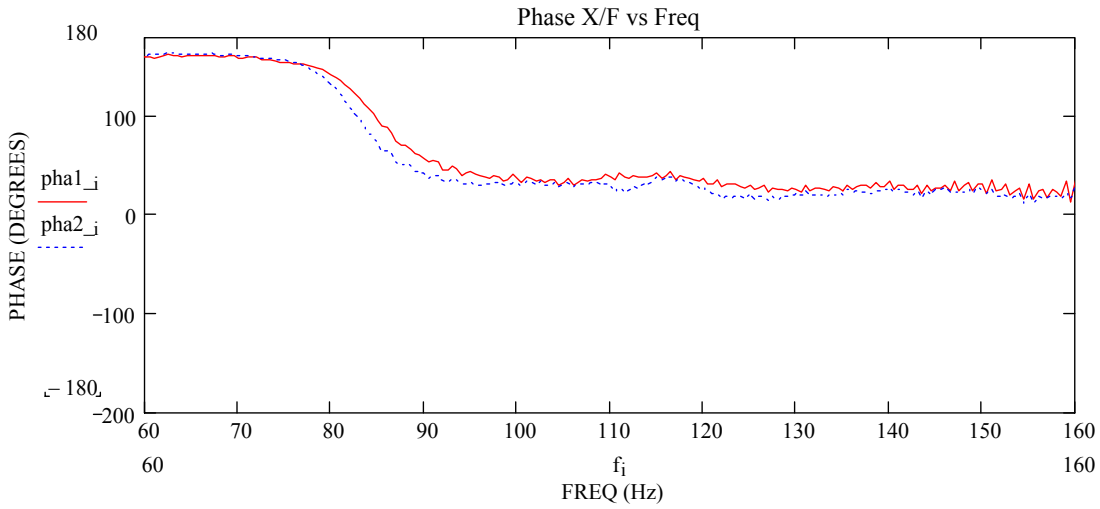

1-whole 2-segmented

Figure 38 Effect of radial segment on transfer function phase

Table 10 Effect of radial segment on the wire mesh coefficients

Sr. No.	Stiffness K		Damping C		%Change
	LB/in	N/m	lb.-sec/in	N-sec/m	
Full Mesh (N)	4820	8.44E+05	1.1375	199.06	13.90
Segmented (S)	4040	7.07E+05	0.94	164.50	17.37

The transfer function plots in Figures 37 and 38 indicate that there is some decrease in the coefficients when the segmented mesh is used. Table 10 shows the percentage decrease in the value of stiffness and damping when the segmented mesh is used. These results are encouraging because even a segment of mesh shows an appreciable amount of damping.

MODELING OF WIRE MESH

Damping Mechanism in Wire Mesh

One of the possible damping mechanisms existing in wire mesh is friction. Okayasu et al. [7] refer to the wire mesh damper they used, as a ‘friction damper’ and reported use of approximate expressions for the equivalent viscous damping. The wire mesh damping increases on the application of external forces like radial or axial compression. Damping decreases with continuous vibration over time and varies with frequency and displacement. All of these suggest that the damping may be due to sliding friction between the wires. On the other hand, amplitude does not become infinite at the resonance as indicated by the vibration model with friction damping [2]. Though there is a very small decrease in measured damping with lubrication [2], it is not equivalent to a significant decrease in the friction coefficient. This suggests that there is more than one damping mechanism present in wire mesh.

Zarzour [3] indicated that damping might be due to hysteresis. Static force displacement curves by Al-Khateeb [2] showed obvious hysteresis in the wire mesh. Another feature, which indicates hysteretic damping, is the non-zero phase angle at zero frequency, which was observed in all the tests done on wire mesh. But the imaginary part of the transfer function not being constant at higher frequencies refutes the hysteretic damping model.

The simplest linear model, which fits the transfer function very well, is a viscous damping model, though there seems to be no possible source of viscous damping in the wire mesh.

Analogy Between Elastomers (Rubbers) and Wire Mesh

In the past few decades, elastomers (rubber) have found extensive use in the industry as a damping material. Over the years, a lot of tests were done to analyze the behavior of elastomers and predict the stiffness and damping coefficients. The data collected was used to form design guidelines [11] for use of elastomers. The behavior of an elastomer as a damping material is very similar to that observed for wire mesh; both of them are nonlinear in nature, both have damping as some combination of coulomb, viscous and hysteretic damping. Thus if we are able to understand the behavior of rubber and the design procedure used, we can develop a similar method to design wire mesh. Appendix A provides a brief overview of the design procedure used for Elastomers. The design procedure described has been adapted from Darlow [11]. The latter part of the Appendix A discusses how a similar approach can be used to develop a design procedure for wire mesh. The elastomer theory was modified by eliminating the effects of shear to make it applicable to wire mesh.

Discussion of the Previous Excel Worksheet

Zarzour [3] numerically solved a stiffness formula, given in equation (11), which uses an equivalent modulus of elasticity (E) obtained from static force-displacement measurements of a wire mesh element. Once this parameter (E) is known, the stiffness can be predicted for elements made of the same wire mesh but of different dimensions, assuming all operational parameters are unchanged. The closed form solution of this equation is given in Equation (12), where L, δ, R_i and R_o refer to axial thickness, radial displacement (X) and inner and outer radii. With shear removed it reduces to equation (12), which is in the worksheet for stiffness as explained by Al-Khateeb [2].

$$K_{xx}=K_{yy} = \frac{2 \cdot E \cdot L \cdot R_i}{\delta \cdot (R_o - R_i)} \int_0^{\pi/2} (\delta \cdot \sin^2\theta - R_i \cdot \sin\theta + \sin\theta \cdot \sqrt{R_i^2 - \delta^2 \cdot \cos^2\theta})\, d\theta \qquad (11)$$

$$K_{xx}=K_{yy}=\frac{2\cdot E\cdot L\cdot R_i}{\delta\cdot(R_o-R_i)}\left[\delta\frac{\pi}{4}-R_i+\frac{1}{2}\sqrt{R_i^{\,2}-\delta^2}+\frac{R_i^{\,2}}{2\cdot\delta}\sin^{-1}\left(\frac{\delta}{R_i}\right)\right] \tag{12}$$

$$K_{xx}=K_{yy}=\frac{2\cdot E\cdot L\cdot R_i}{\delta\cdot(R_o-R_i)}\left[\delta\frac{\pi}{4}+\frac{1}{2}\sqrt{R_i^{\,2}-\delta^2}-\frac{R_i}{2}\right] \tag{13}$$

Experiments done by Al-Khateeb indicate that the above formula (13) needs to be modified to include effect of other parameters like dynamic strain and frequency.

Modeling of Wire Mesh

Al-Khateeb [2] showed that damping in wire mesh can not be modeled just by using one mechanism. It has to be some combination of viscous, hysteretic and coulomb damping, even though the viscous damping mechanism has no known source in wire mesh. He also showed that nonlinear models predict better results than the linear ones. A stick-slip model is given in Appendix B as a possible damping mechanism.

Analysis of the forced vibrations of a SDOF system with both viscous and coulomb damping is given in the classical work by Den Hartog [12]. The model has limitations at low frequency ratios since it is based on continuous motion (without stops). This model produces promising results that generally predict the behavior of wire mesh shaker test transfer functions. However, modifying the viscous damping coefficient in the model, by using the concept of equivalent damping(C = H/Ω) produces even better results.

The model for stiffness and damping first proposed by Zarzour [3] is actually the elastomer model with shear removed, as follows:
The complex stiffness model for a 1-DOF system is given in equation 14.

$$m\ddot{x}+k\left(1+\frac{h}{k}i\right)x=0 \tag{14}$$

The loss coefficient (β) is defined here as the hysteretic coefficient (h) divided by the stiffness (*k*). Equation 15 gives this expression.

$$\beta = \frac{h}{k} \tag{15}$$

The loss coefficient β can be determined from time response data by measuring the logarithmic decrement (logdec) δ. Equation 16 gives an expression for the loss coefficient β as a function of the logdec (δ).

$$\beta = \frac{2(e^{\delta} - 1)}{\pi(e^{\delta} + 1)} \tag{16}$$

The loss coefficient can also be calculated from shaker tests. The imaginary part of the transfer function F/X gives "h = kβ" lb/in where the slope is zero.

The following discussion considers the effect of parameters like amplitude, frequency, radial thickness, axial thickness, radial interference and axial compression on stiffness and damping of wire mesh bearing damper and tries to provide a relation for them. An equivalent viscous damping coefficient was used, as it fits the data very well and is easy to calculate and compare. MathCAD worksheets were developed to curve fit the data with separate expressions and effort was made to keep the expressions as simple as possible. Table 11 shows the expressions derived for the various parameters.

Table 11 Expressions obtained for damping and stiffness coefficients

Parameter	Stiffness (lbs./in)	Damping(lbs.-sec/in)
Radial Thickness	1160*(Ro+Ri)/(Ro-Ri)	0.31*(Ro+Ri)/(Ro-Ri)
Axial Compression	4912 *(1+1.6E-04*AC^2)	1.076*(1+3.51E-04*AC^2)
Radial Interference	4816*(1+19.5E-03*RI)	1.13*(1+9.73E-03*$RI^{1.5}$)
Disp. Amplitude	3882*(1+0.148*$Amp^{-2/3}$)	0.548*(-1+2.087*$Amp^{-2/3}$)

The above expressions and results obtained in the last section can be combined to give equation (17) and (18)

$$\text{Stiffnes} := \text{Const1}\cdot f(L)\cdot f(Ro,Ri)\cdot f(AC)\cdot f(RI)\cdot f(Amp)$$
$$\text{Damping:} = \text{Const2}\cdot g(L)\cdot g(Ro,Ri)\cdot g(AC)\cdot g(RI)\cdot g(Amp) \tag{17}$$

$$K := \text{Const1}\cdot\frac{Ro+Ri}{Ro-Ri}\cdot\left(1+1.6\cdot10^{-4}\cdot AC^2\right)\cdot\left(1+19.5\cdot10^{-3}\cdot RI\right)\cdot\left(1+0.148\cdot Amp^{\frac{-2}{3}}\right)\cdot L$$
$$C := \text{Const2}\cdot\frac{Ro+Ri}{Ro-Ri}\cdot\left(1+3.5\cdot10^{-4}\cdot AC^2\right)\cdot\left(1+9.73\cdot10^{-3}\cdot RI\right)\cdot\left(1+0.682\cdot Amp^{\frac{-2}{3}}\right)\cdot L \tag{18}$$

Al-Khateeb [2] derived expression for the effect of frequency, which can be used, provided the constants are different.

After the inclusion of all the effects the worksheet can be modified with the following new expressions

$$K := Const1\cdot\frac{Ro + Ri}{Ro - Ri}\cdot\left(1 + 1.6\cdot10^{-4}\cdot AC^{2}\right)\cdot\left(1 + 19.5\cdot10^{-3}\cdot RI\right)\cdot\left(1 + 0.148\cdot Amp^{\frac{-2}{3}}\right)\cdot L\cdot(1.0002)^{om}$$

$$C := \frac{Const2}{om}\cdot\frac{Ro + Ri}{Ro - Ri}\cdot\left(1 + 3.5\cdot10^{-4}\cdot AC^{2}\right)\cdot\left(1 + 9.73\cdot10^{-3}\cdot RI^{1.5}\right)\cdot\left(1 + 0.682\cdot Amp^{\frac{-2}{3}}\right)\cdot L\cdot(fr)^{\frac{-4}{5}} \quad (19)$$

Const1 is the Equivalent Young's modulus (E_{eq}) for that wire mesh material. The term equivalent is used because the actual Young's modulus of the material would be different than the one for a donut made of wire mesh. Const2 is the Equivalent Hysteretic Damping Coefficient (H) which can be calculated from tests done on a sample wire mesh element. The previous worksheet developed by Zarzour [3] assumes a guess value of Equivalent Young's Modulus, matches it with the measured stiffness and then gives the prediction for a mesh of different geometry. The procedure has been modified in the present research and is explained in the next section.

In the above equations the subfunctions involving axial compression, radial interference, displacement amplitude and axial thickness are not dimensionless. This may lead to some concerns for the application of the same equations for wire mesh of very large or very small dimensions and having large variation in test conditions. The above equations were nondimensionalized so that a more general solution can be obtained. Some of the functions are interdependent hence the equations cannot be directly converted to nondimensional form. Certain curve fits were varied and the best fit was obtained using the equations (20). Here om indicates the frequency of vibration.

$$K := Const1\cdot\frac{L}{Ro - Ri}\cdot\left[1 + 4\cdot10^{-5}\cdot\left(\frac{AC}{L}\right)^{2}\right]\cdot\left[1 + 29.62\cdot10^{-3}\cdot\left(\frac{RI}{Ro - Ri}\right)\right]\cdot\left[1 + 0.112\cdot\left(\frac{Amp}{Ro - Ri}\right)^{\frac{-2}{3}}\right]\cdot(1.0002)^{om}$$

$$C := \frac{Const2}{om}\cdot\frac{L}{Ro - Ri}\cdot\left[1 + .875\cdot10^{-4}\cdot\left(\frac{AC}{L}\right)^{2}\right]\cdot\left[1 + 18\cdot10^{-3}\cdot\left(\frac{RI}{Ro - Ri}\right)^{1.5}\right]\cdot\left[1 + 0.5182\cdot\left(\frac{Amp}{Ro - Ri}\right)^{\frac{-2}{3}}\right]\cdot(fr)^{\frac{-4}{5}} \quad (20)$$

The above equations were extracted by varying one parameter at a time. To ensure that these equations apply to the case where there is a variation in all the parameters at the same time, tests were conducted on a wire mesh of different dimensions and different test conditions. Following Table 12 shows the results of the testing.

Table 12 Comparison of measured and predicted results

Rad Thick	Rad Int	Axial Comp	Amp	K meas	K pred	%Error	C meas	C pred	%Error
inches	mils	mils	mils	lb/in	lb/in		lb-sec/in	lb-sec/in	
0.760	0	0	1	7730	7547	2.3674	1.27	1.25	1.5748
0.760	3	40	0.5	11056	10780	2.4964	3.12	3.108	0.3846
0.760	6	0	0.5	9289	8968	3.4557	2.17	2.4	-10.6
0.760	6	20	0.5	9883	9950	-0.678	2.48	2.57	-3.629
0.760	6	40	0.5	11667	11810	-1.226	3.39	3.263	3.7463
0.760	6	40	0.25	12971	12200	5.944	4.82	5.015	-4.046

DESIGN PROCEDURE

The following section provides a simple and ready to use tool for engineers, to design wire mesh as a bearing damper. The empirical non-dimensional equations were used to predict the stiffness and damping coefficients of the wire mesh bearing damper. An Excel workbook was developed, to enable the user to design wire mesh dampers for use in real machinery. The user is provided with following two options in the Excel workbook:

Design Using Existing Wire Mesh Material

Extensive testing was done on wire mesh made of copper wire, 0.0126in in diameter, having Jersey-stitch design, commercially available from Metex Corporation. The required design data, for use of wire mesh made from this material, was collected in the present research. With the help of the present Excel sheet called "design", the user can obtain the stiffness and damping characteristics of the wire mesh by specifying the geometric requirements and operating conditions. The sheet asks for the following input data:

- Outer radius of the mesh Ro,
- Inner radius of the mesh Ri,
- Axial Length of the mesh L,
- Maximum Amplitude of Vibration Amp,
- Axial compression AC,
- Radial Interference RI,
- Frequency ω,
- Natural frequency ω_n

The worksheet then provides the user with the stiffness and damping values of the wire mesh subject to the above conditions.

Design Using Alternative Wire Mesh Material

Materials other than copper mesh and of different wire diameter can be used for wire mesh design but require some preliminary testing. The following would be the determining factors for the design of wire mesh:

- The "Target" or desired WMD stiffness coefficient from a rotordynamic model (XLTRC) of the turbomachine.
- The "Target", or desired WMD damping coefficient from a rotordynamic model (XLTRC) of the turbomachine,
- The maximum overall displacement (0-pk) at the location of the WMD, predicted by the XLTRC.
- The frequency (rad/s) at which the maximum displacement occurs, predicted by the XLTRC.
- The Natural frequency as predicted by the XLTRC.

A donut of the desired wire mesh material (but not necessarily of the desired dimensions) must be purchased and tested. Certain sizes are economically available "off the shelf". A transfer function shaker test needs to be done on the sample wire mesh element. Periodic chirp excitation should be used and force-displacement data should be collected using a two-channel analyzer. Amplitude and Phase of the Transfer function (X/F) can be directly obtained from the analyzer and can be used to calculate the stiffness and damping values. These values and the various parameters from the test are to be used in the "constants" worksheet, to calculate the Equivalent Young's modulus and the Equivalent Hysteretic damping coefficient, for that particular material. These calculated constants can then be used in the "design" sheet of the Excel workbook for calculation of the stiffness and damping for the desired wire mesh donut.

The following Figures 39 and 40 show the two design worksheets and a sample input/output. Figures 41 and 42 show the help sheets included in the code.

Wire Mesh Design

Outer Radius	Ro	3.46	inches
Inner Radius	R	1.96	inches
Axial Thickness	L	0.5	inches
Axial Compression	AC	0	mils
Radial Interference	RI	0	mils
Max Amplitude	Amp	0.5	mils
Frequency	Omega	90	Hz
Natural frequency	OmegaN	76	Hz

Equivalent Young's modulus	E'	10500	lb./in^2
Eqv. Hysteretic Damping Coeff	H'	1020	lb/in

K = 4832.14 lb/in

C = 1.09092 lb-sec/in

For Cu Mesh of wire diameter 0.0126in and 42.7% density
Eqv. Young's modulus=10500 lb/in^2, Eqv. Hysteretic Damping Coeff=1020 lb/in

Need Help?

Figure 39 Design worksheet

Sheet to Calculate Constants for an Alternate Wire Mesh Material

Sample Donut Parameters:

Stiffness	K	4829	lb/in			
Damping	C	1.08	lb-sec/in			
Outer Radius	Ro	3.485	inches			
Inner Radius	R	1.96	inches			
Axial Thickness	L	0.5	inches			
Max Amplitude	Amp	0.5	inches	Eqv. Young's Modulus E'	10645.78	lb./in^2
Frequency	Omega	90	Hz			
Natural Frequency	OmegaN	76	Hz	Eqv. Hysteretic Coeff. H'	1020.749	lb/in

Need Help?

Figure 40 Constants worksheet

Help for "Design" Sheet

Back to Design Sheet

This worksheet calculates the stiffness and damping coefficients for a wire mesh donut having the inputed design, installation and operational parameters.
The sheet will calculate the coefficients for the material whose Equivalent young's modulus, E' and Equivalent hsteretic damping coeff., H' are already known. If an alternative wire mesh material is to be used, E' and H' should be first determined from the "constants" worksheet and then these values should be used in the present worksheet to find the stiffness and damping values for that material.

The sheet requires following Input:

* **Ro** the Outer Radius of the wire mesh donut to be used.
* **R** the Inner Radius of the wire mesh donut.
* **L** the Axial Length of the wire mesh donut.
* **AC** the Axial Compression applied to the length of the donut.
* **RI** the Radial Interference applied to the donut.
* **Amp** the Maximum Amplitude of Vibration occuring at the wire mesh location.
* **Omega** the frequency in Hz. at which the value of the coefficients is desired.
* **OmegaN** the natural frequency in Hz. of the test rig (either standard or measured as in constants worksheet).
* **Equivalent Young's modulus** of the donut material either used for the standard material (Cu wire of diameter 0.0126" and 42.7% in density) or calculated from the constants worksheet.
* **Eqv. Hyseteretic Damping Coeff** of the donut material either used for the standard material (Cu wire of diameter 0.0126" and 42.7% in density) or calculated from the constants worksheet.

The worksheet then calculates the Stiffness and Damping coefficients for the above wire mesh geometry and test conditions.

Back to Design Sheet

Figure 41 Help for design worksheet

Help for "Constants" Sheet

Back to Constants Sheet

This worksheet is to be used for the design of wire mesh having material different from the one tested A&M. It calculates the value of the Eqv. Young's modulus, E' and Eqv. Hysterestic Damping Coeff., H', in the "design" worksheet to calculate

This requires a simple shaker test to be conducted on a Sample wire mesh donut made of the material having the dimensions comparable to the size which is expected to be used in the

The sheet requires following

* **K** the measured stiffness coefficient of the Sample wire
* **C** the measured damping coefficients of the Sample wire
* **Ro** the Outer Radius of the Sample wire mesh
* **R** the Inner Radius of the Sample wire mesh
* **L** the Axial Length of the Sample wire mesh
* **Am** the Maximum displacement measured during the test at wire
* **Omega** the measured frequency of
* **OmegaN** the measured natural frequency of the test

The worksheet than calculates the values of E' and H' for that particular wire mesh material. These "Design" worksheet to find K and C for this wire mesh material donut having different operational

Back to Constants Sheet

Figure 42 Help for constants worksheet

SUMMARY AND CONCLUSIONS

Seven major groups of experiments on wire mesh bearing dampers were conducted, using a non-rotating test rig. The wire mesh is in the form of a donut to fit around the outer race of a ball bearing, or around the shell of a fluid film bearing. Two different axial thicknesses and four different radial thicknesses of wire mesh were tested. All the other test parameters, namely axial compression, radial interference and displacement amplitude were maintained at the same level, such that only the effect of change in axial thickness and subsequently radial thickness was observed. Both stiffness and damping were found to be directly proportional to the change in axial thickness. Stiffness and damping exhibited an inverse relationship with radial thickness, which was quantified by curve-fitting the data in MathCad. Twelve axial compression levels were tested and the extracted coefficients were curve fitted using a second order polynomial. Similar tests were done for eight values of radial interference and seven values of displacement amplitude. The displacement amplitude was limited due to the maximum force that can be applied with the shaker. In all the above tests, the primary objective was the quantification of effect of various parameters, which required collection of a large number of meaningful data points. A mesh having two splits was tested and compared with mesh without any splits and was found to have very small decrease in stiffness and damping. Another very interesting result came out of testing a mesh comprising of two segments and comparing it against tests from a complete donut. It was observed that the segmented mesh retained an appreciable amount of stiffness and damping. This mesh was very easy to install and allowed a lot of free space in between the two segments. Another advantage was that it could sustain reasonable error in the inner/outer radius, as it was not constrained at the sides and could flex.

Design expressions were obtained for the various parameters, using the curve-fitting features in MathCad^{TM}. A product solution was assumed and the combined effect of all the parameters was used to modify the existing design worksheet. To make the expressions more general, the equations for stiffness and damping were non-

dimensionalized. A comprehensive ready-to-use design guideline was provided for the wire mesh dampers. The design guide provides two design scenarios, one for the design of wire mesh made of the same material and density as already tested in the laboratory (in the present work), and the second for design of wire mesh dampers using an alternative wire mesh material. The second design procedure requires some transfer function tests to be done on a sample wire mesh donut, following which the worksheet is capable of giving coefficients for different design and test conditions. The Excel worksheet is capable of predicting stiffness and damping for a wire mesh donut subject to changes in the following parameters: radial thickness, axial thickness, axial compression, radial interference, displacement amplitude and frequency. The sheet can be used as an effective tool to design wire mesh bearing dampers for turbomachinery applications.

REFERENCES

[1] Wang, X., and Zhu, Z., 1997, "Ring-like metal rubber damper", Hangkong Dongli Xuebao/Journal of Aerospace Power, **12**(2), pp. 143-145.

[2] Al-Khateeb, E. M., 2002, *Design, Modeling and Experimental Investigation of Wire Mesh Vibration Dampers*, Unpublished PhD. dissertation, Department of Mechanical Engineering, Texas A&M University, College Station.

[3] Zarzour, M. J., 1999, *Experimental Evaluation of a Metal-Mesh Bearing Damper in a High Speed Test Rig*, Unpublished M.S. thesis, Department of Mechanical Engineering, Texas A&M University, College Station.

[4] Childs, D. W., 1978, "The Space Shuttle Main Engine High-Pressure Fuel Turbopump Rotordynamic Instability Problem," ASME Journal of Engineering for Power, **100** (January), pp. 48-57.

[5] Rivin, E., 1979,"Vibration Isolation of Precision Machinery," SV, Sound and Vibration, **13**, n 8, pp. 18-23.

[6] Barnes, A. B., 1984, "Improvement in Machinery for Woven Wire Mesh," Wire Industry, **51**(605), pp. 403-404.

[7] Okayasu, A., Ohta, T., Azuma, T., Fujita, T., and Aoki, H., 1990 "Vibration Problems in the LE-7 Liquid Hydrogen Turbopump," Proceedings of the 26th AIAA Joint Propulsion Conference, Orlando, Florida, pp. 1-5.

[8] Burshid, S. M., 1999, *Experimental Evaluation of Rotordynamic Coefficients for Hybrid Metal Mesh Pocket Damper Seals in Turbomachinery*, Unpublished M.S.

Thesis, Department of Mechanical Engineering, Texas A&M University, College Station.

[9] Al-Khateeb, E.M., and Vance, J.M., 2001, "Experimental Evaluation of a Metal Mesh Bearing Damper in Parallel with a Structural Support," ASME Paper 2001-GT-0247, presented at the ASME Turbo Expo, 4-7, June, 2001, New Orleans, Louisiana.

[10] Ertas, B., Al-Khateeb, E.M., and Vance, J.M., 2002, "Cryogenic Temperature Effects on Metal Mesh Dampers and Liquid Hydrogen Turbopump Rotordynamics," AIAA Paper AIAA-2002-4164, accepted for presentation at the 38th AIAA/ASME/SAE/ASEE Joint Propulsion Conference, 7-10, July, 2002, Indianapolis, Indiana.

[11] Darlow, M. and Zorzi, E., 1981, *Mechanical Design Handbook for Elastomers*, National Aeronautics and Space Administration, NASA CR-3432.

[12] Den Hartog, J. P, 1985, *Mechanical Vibrations*, Dover Publications, New York, NY.

APPENDIX A: DESIGN EQUATIONS FOR ELASTOMERS

Dynamics

Viscoelastic materials combine the properties of purely elastic materials with those of purely viscous materials. For an elastic material there exists a relationship between stress and strain, which in case of linear elastic material is given by Hooke's law. For a linear viscous material stress is directly proportional to the rate of strain. Elastomers mostly follow a near linear viscoelastic behavior. The elastic and viscous moduli for elastomers tend to be a function of frequency, temperature, strain, geometry and material composition.

Basic relationship

When a load cycle is applied repeatedly to an elastomer element, the process of relaxation causes hysteresis. Hysteresis loop results in a loss of energy per cycle equal to the area of the hysteresis loop. Thus elements with hysteretic loop cause energy loss or damping. For such materials the load displacement relationship can be defined as under

$$F=K^*x \tag{20}$$

Where

$$F=F^* e^{i\omega t},\ x =x^* e^{i\omega t},\ K^*=k_1+ik_2$$

F* and x* are complex numbers defining the amplitude and phase of displacement and force variations and only real parts are used to establish values for F and x. K* is referred as complex stiffness and k_1 and k_2 are referred to as stiffness and damping of the element respectively.

Also $K^*= k_1 (1+i\eta)$

Where η is the loss factor defined as

$$\eta= k_2 / k_1 = D/(2*pi*U)$$

D and U are the energy dissipated per cycle and the energy stored at maximum displacement respectively.

Effects of geometry

For a general elastomer element, the geometry can be characterized by a certain area of the element (A) that is stressed and a certain dimension (h), which is strained. Figure A1 shows two-element geometry. For the shear element the stressed area A is its width times its length (b*l) and the strained dimension is its thickness, h. For the compression element, the stressed area is the top area of the cylinder $\pi*d^2/4$ and its strained length is the height, h.

For shear specimen

$k_1 = G'_{eff} A/h$ (21a)

$k_2 = G''_{eff} A/h$ (21b)

where G'_{eff} and G''_{eff} are shear moduli also called effective storage and loss moduli.

For compression specimen

As $E=2(1+\nu)G$ where Poisson's ratio 'ν' for most elastomers is 0.4945 to 0.4999

$k_1 = 3G'_{eff} A/h$ (22a)

$k_2 = 3G''_{eff} A/h$ (22b)

G'_{eff} and G''_{eff} are effective moduli and are functions of material, frequency, amplitude, temperature, initial strain and the geometry.

For static loading the effects of bending can be shown to cause following relationship for shear element

$$(G'_{eff})_{static} = G'_{static} /(1 + h^2/3l^2) \quad (23)$$

For a compression element the relation is

$$(G'_{eff})_{static} = G'_{static}(1+\beta.S^2) \quad (24)$$

$$k_1 = 3 (A/h)*G'_{static}(1+\beta'.S^2) \quad (25a)$$

$$k_2 = 3 (A/h)*G''_{static}(1+\beta''.S^2) \quad (25b)$$

where β' and β'' are known as shape factor which depend on frequency, temperature and dynamic strain.

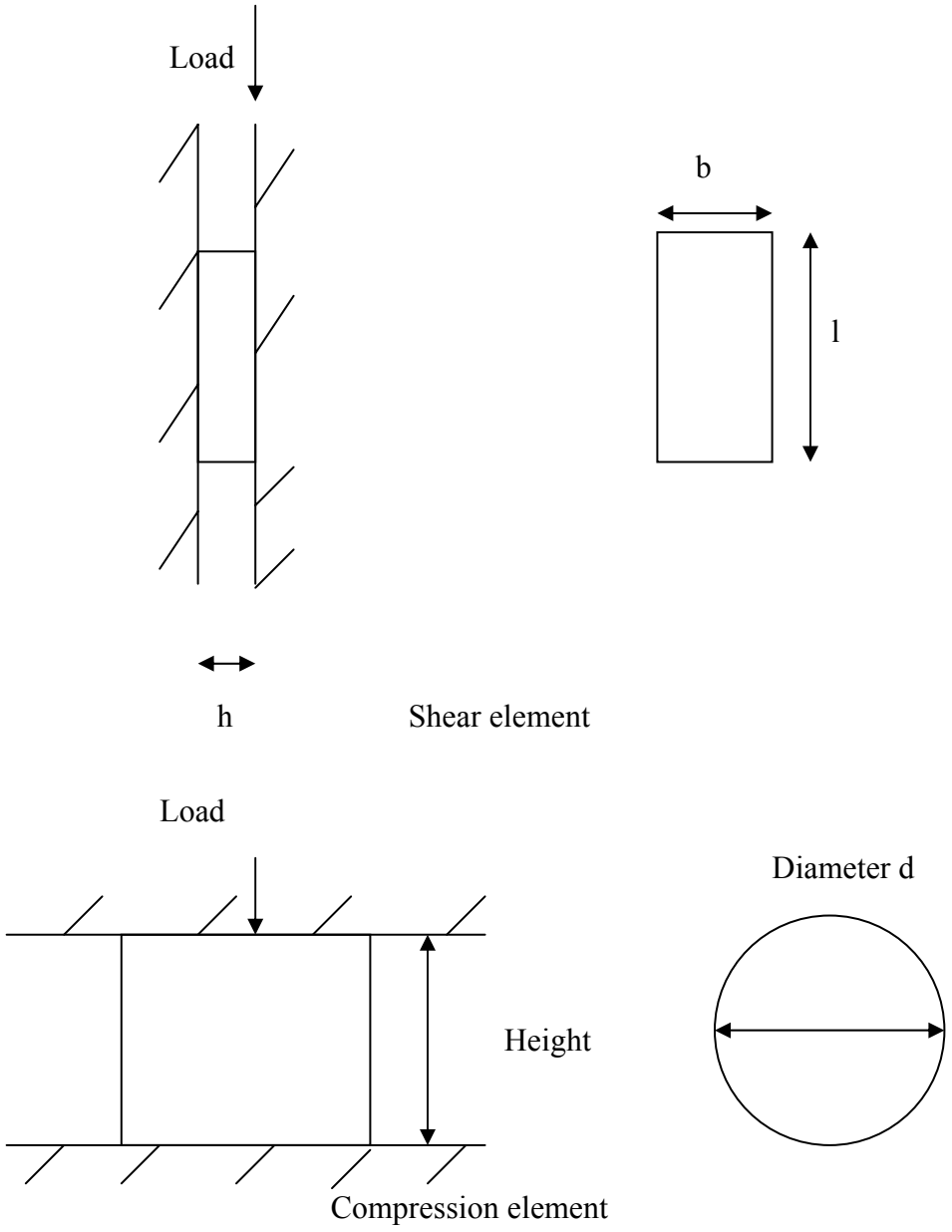

Figure A1 Element geometries

Where l is the dimension of the sheared area in the direction parallel to the loading.

S is the ratio of the loaded area to the unloaded area and is referred to as geometric factor.

In practice more complex elastomer geometries are used which can be considered by following methods.

1) Beamcolumn method
2) Method of Gobel
3) Plane stress analysis.

For a donut of outer radius Ro, inner radius Ri, thickness L, and shear modulus G, Beam column method gives the coefficients as

$k_1=2\pi G'L(R_o+R_i)/(R_o-R_i)$ 26(a)

$k_2=2\pi G''L(R_o+R_i)/(R_o-R_i)$ 26(b)

Effect of frequency and temperature

The effects of temperature and frequency on the shear moduli are inversely related and may be represented by a single independent variable. Reduced shear moduli are used as given by

$G'_r = G' T_c/T$ (27a)

$G''_r = G'' T_c/T$ (27b)

Where G'_r and G''_r are the reduced shear storage and loss moduli, T_c is the characteristic temperature of the particular elastomeric material and T is the temperature of the elastomer element.

Effect of static and dynamic strain

Static strain has a significant effect on the dynamic properties of elastomers only if its magnitude is too large which is only in case of complex geometries like O-rings. For simple geometries the effect of modest preload (< 5%) the effect is very small. On the

other hand the effect of dynamic strain is very pronounced and is mainly dependent on chemical and thermal factors.

Formulation of equations

Assuming that the effects of strain and reduced frequency can be separated, the reduced shear moduli are given by

$$G'_r = f'(\alpha_T \omega) \cdot g'(\varepsilon) \quad (28a)$$

$$G''_r = f''(\alpha_T \omega) \cdot g''(\varepsilon) \quad (28b)$$

f( ), g( ) represent unknown functions, $(\alpha_T \omega)$ is the reduced frequency , and ε is the dynamic strain. The coefficient α_T is determined from

$$\log_{10}\alpha_T = C1(T-T_c)/(C2+T-T_c) \quad (29)$$

where C1 and C2 depend on the elastomer composition given in Table A1.

Table A1 Values for C1, C2 and characteristic temperature T_c

Elastomer Material	C1	C2	Tc
Butadiene (polybutadiene)	-7.48	90.7	268.1
Fluorocarbon (Viton)	-8.86	101.6	306
Nitrile (Buna-N)	-8.86	101.6	293
Chloroprene (Neoprene)	-8.86	101.6	272
EPDM	-8.86	101.6	267

The logarithms of the shear moduli have been shown to vary approximately linearly with the logarithms of the frequency. Thus

$$f'(\alpha_T\omega) = a_1 \ (\alpha_T \ \omega)^{a}{}_2 \quad (30a)$$

$$f''(\alpha_T\omega) = b_1 \ (\alpha_T \ \omega)^{b}{}_2 \quad (30b)$$

where a and b are constants determined empirically for a particular elastomer material.

The logarithms of shear moduli also have been shown to posses a quadratic relationship to the logarithm of the dynamic strain. Thus,

$$\log_{10}g'(\varepsilon) = a_3 + a_4\log_{10}\varepsilon + a_5(\log_{10}\varepsilon)^2 \quad (31a)$$

$$\log_{10} g''(\varepsilon) = b_3 + b_4 \log_{10}\varepsilon + b_5 (\log_{10}\varepsilon)^2 \quad (31b)$$

thus,

$$g'(\varepsilon) = a'_3 \varepsilon^{a_4 + (a_5 \log_{10}\varepsilon)} \quad (32a)$$

$$g''(\varepsilon) = b'_3 \varepsilon^{b_4 + (b_5 \log_{10}\varepsilon)} \quad (32b)$$

From equations 28 and 32,we get

$$G'_r = a_6 (\alpha_T \omega)^{a_2} \varepsilon^{a_4} \varepsilon^{(a_5 \log_{10}\varepsilon)} \quad (33a)$$

$$G''_r = b_6 (\alpha_T \omega)^{b_2} \varepsilon^{b_4} \varepsilon^{(b_5 \log_{10}\varepsilon)} \quad (33b)$$

The relation for the original shear moduli can be given by equations

$$G' = (T/T_c) a_6 (\alpha_T \omega)^{a_2} \varepsilon^{a_4} \varepsilon^{(a_5 \log_{10}\varepsilon)} \quad (34a)$$

$$G'' = (T/T_c) b_6 (\alpha_T \omega)^{b_2} \varepsilon^{b_4} \varepsilon^{(b_5 \log_{10}\varepsilon)} \quad (34b)$$

The above equations can be made linear by taking the logarithm of both sides.

$$\log_{10}(G' T_c/T) = a_7 + a_2(\log_{10}\alpha_T + \log_{10}\omega) + a_4 \log_{10}\varepsilon + a_5(\log_{10}\varepsilon) \quad (35a)$$

$$\log_{10}(G'' T_c/T) = b_7 + b_2(\log_{10}\alpha_T + \log_{10}\omega) + b_4 \log_{10}\varepsilon + b_5(\log_{10}\varepsilon) \quad (35b)$$

Thus, once sufficient amount of experimental data has been generated for a particular elastomer material, the unknown coefficients of equations 34a and 34b can be found using a standard statistical regression analysis. The value of these coefficients is determined for four different elastomers, and presented in Table A2 & A3.

Now the only unknowns in equation 25a and 25b are β' and β''. Thus we can rewrite those equations as

$$\beta' = (k'_c h/(3G'A) - 1)(4t/D)^2 \quad (36a)$$

$$\beta'' = (k''_c h/(3G''A) - 1)(4t/D)^2 \quad (36b)$$

Then using the results of compression specimen tests relations for β' and β'' as functions of frequency, temperature and strain can be found using statistical regression analysis. The relationships are again logarithmic and given by

$$\log_{10}\beta' = d_1 + d_2\log_{10}\omega + d_3\log_{10}(T/T_c) + d_4\log_{10}\varepsilon \quad (37a)$$

$$\log_{10}\beta'' = e_1 + e_2\log_{10}\omega + e_3\log_{10}(T/T_c) + e_4\log_{10}\varepsilon \quad (37b)$$

$$\beta' = 10^{d1}.\ \omega^{d2}.(T/T_c)^{d3}.\ \varepsilon^{d4} \quad (38a)$$

$$\beta'' = 10^{e1}.\ \omega^{e2}.(T/T_c)^{e3}.\ \varepsilon^{e4} \quad (38b)$$

The values of coefficients in the above equation for butadiene are given in Table A4.

Thus given the Area of Cross Section A, length h, material, frequency ω, dynamic strain ε and temperature T, the values of stiffness and damping coefficients can be calculated using the design equations given above and by utilizing the data collected by experimentation.

Table A2 Regression coefficients for dynamic shear storage moduli

Elastomer Material	$a_7=\log_{10}a_6$	a_2	a_4	a_5	Std.dev (σ)
Butadiene(polybutadiene)	5.73±.03	0.192±.004	-0.746±.030	-0.129±.007	0.0266
Fluorocarbon(Viton)	6.31±.04	0.419±.005	-0.115±.031	-0.0159+.005′	0.0527
Nitrile(Buna-N)	6.19±.02	0.124±.002	-0.148±.017	-.0209±.0035	0.0211
Chloroprene(Neoprene)	6.18±.01	.0911±.0041	-0.273±.012	-0.0424±.002(	0.0103
EPDM	5.65±.04	0.141±.005	-.838±.034	-0.137±.007	0.0329

Table A3 Regression coefficients for dynamic shear loss moduli

Elastomer Material	$b_7=\log_{10}b_6$	b_2	b_4	b_5	Std.dev (σ)
Butadiene (polybutadiene)	5.48±.06	0.242±.008	-0.387±.06	-0.0872±.01	0.0544
Fluorocarbon (Viton)	5.31±.05	0.389±.006	-0.135±.04	-0.0179+.00	0.0676
Nitrile (Buna-N)	5.53±.07	0.290±.007	0	0	0.0680
Chloroprene (Neoprene)	5.58±.04	0.197±.012	-0.132±.03	-0.0289±.00	0.0314
EPDM	5.78±.07	0.154±.009	-.223±.060	-0.0553±.01	0.0583

Table A4 Regression coefficients for dynamic storage and loss shape factor from Polybutadiene compression tests

Subscript	Storage Shape Factor d	Loss Shape Factor e
1	0.615±0.175	0.884±0.145
2	- 0.142±0.049	-0.180±0.041
3	2.13±0.32	1.29±0.27
4	-0.0837±0.0148	-0.101±0.012

APPENDIX B: STICK SLIP MODEL TO EXPLAIN THE DAMPING

A stick-slip model was presented in by Al-Khateeb [2] as a possible damping mechanism. Based on this model, the wire mesh can be imagined to be composed of a number of stick-slip joints. As the displacement (or force) increases, some of the joints are freed resulting in a series combination of wires. A series combination, such as in Figure A2, produces lower equivalent stiffness and damping values.

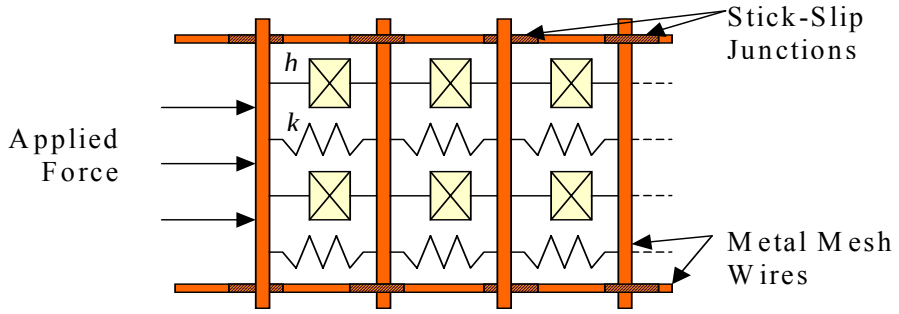

Figure A2 Wire mesh stick-slip (SS) model

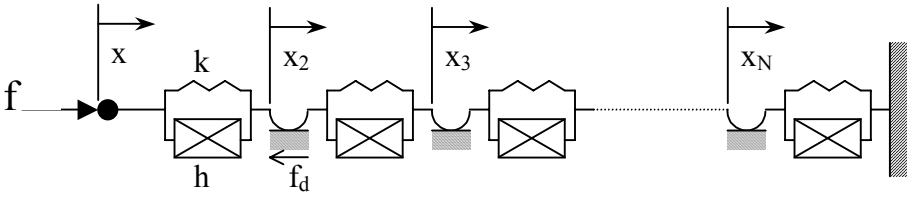

Figure A3 One row of wire elements in the stick-slip (SS) model

Figure A3 shows a row of N elements (spring-damper combinations) in a simplified model incorporating stick-slip friction between the wires. The mass of each wire is insignificant compared to the system mass, and will be neglected in this model. In

addition, dynamic motion (no stops) and constant friction force at the joints (f_d) are assumed in this analysis. For slip motion of the first two elements (i.e., only two elements are free to move) to the right, we can write the following equations of motion based on the complex-stiffness model.

$$F - k \cdot (1+i\cdot\beta) \cdot (X-X_2) = 0 \tag{14}$$

$$k \cdot (1+i\cdot\beta) \cdot (X-X_2) - f_d - k \cdot (1+i\cdot\beta) \cdot X_2 = 0 \tag{15}$$

In these equations, the constants k, β and f_d represent stiffness, loss coefficient (h/k) and friction force for each element, respectively. Eliminating X_2 in the above equations and rearranging we get the following expression.

$$F/X = k \cdot (1+i\cdot\beta) / (2 - f_d /F) \tag{16}$$

Working with more elements, we soon realize the general expression for n number of slipping or 'participating' elements ($n \leq N$) up to the maximum force. The expression is given in Equation (17) below, where P is the friction-to-excitation force ratio (f_d/F). For a model with friction at the first element, the expression remains the same except that R is replaced with (R + 1).

$$\frac{F}{X} = \frac{k \cdot (1 + i \cdot \beta)}{n \cdot (1 - R \cdot P)} \quad , \quad R = \frac{\sum_{j=0}^{n-1} j}{n} \tag{17}$$

Applying the above equation to a wire mesh element would account for only one axial layer, with series elements in the radial direction. The number of elements in this layer (N) is estimated by $4 \cdot Vr \cdot Rt/(\pi \cdot d_w)$, truncated to an integer, where Rt is the radial thickness and d_w is the wire diameter. Here, Vr is equal to the sum of wire cross-

sectional areas divided by wire mesh element cross-sectional area, hence equaling density of the wire mesh element. In order to represent the entire wire mesh element, the above expression is multiplied by the number of layers, giving Equation (18), where T is the axial thickness. The number of layers is roughly equal to the number of elements per cross-section divided by N.

$$\frac{F}{X} = \frac{T}{d_w} \cdot \frac{k \cdot (1 + i \cdot \beta)}{n \cdot (1\text{-}R \cdot P)} \tag{18}$$

In addition to predicting increasing coefficients with thickness and density, the SS model predicts higher coefficients at smaller wire diameters, assuming k and β unchanged. This may explain the stiffness and damping values reported by Burshid [8] for wire mesh elements of lower wire diameter and axial thickness, which were on the order of measurements by Zarzour [3] and Al-Khateeb [2]. We should also note that the force dependency of the SS model coefficients is attributed to the dependency of n and P on F. In fact, n is the lowest integer satisfying $n \cdot P \geq 1$, as seen from Equation (19) below.

$$F - (n - 1) \cdot f_d \leq f_d \Rightarrow P^{-1} - (n - 1) \leq 1 \Rightarrow n \cdot P \geq 1 \tag{19}$$

Amplitude dependency of coefficients in the SS model is shown in Figure A4. In Figure A5, the model is compared to static force-displacement measurements for wire mesh element N4. However, this model stops short of explaining frequency, radial thickness and temperature effects.

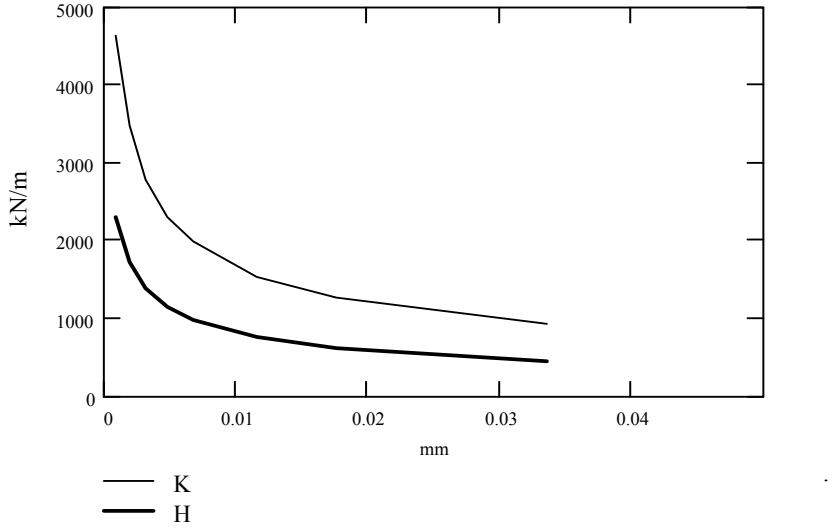

Figure A4 Amplitude dependency of coefficients in the SS model

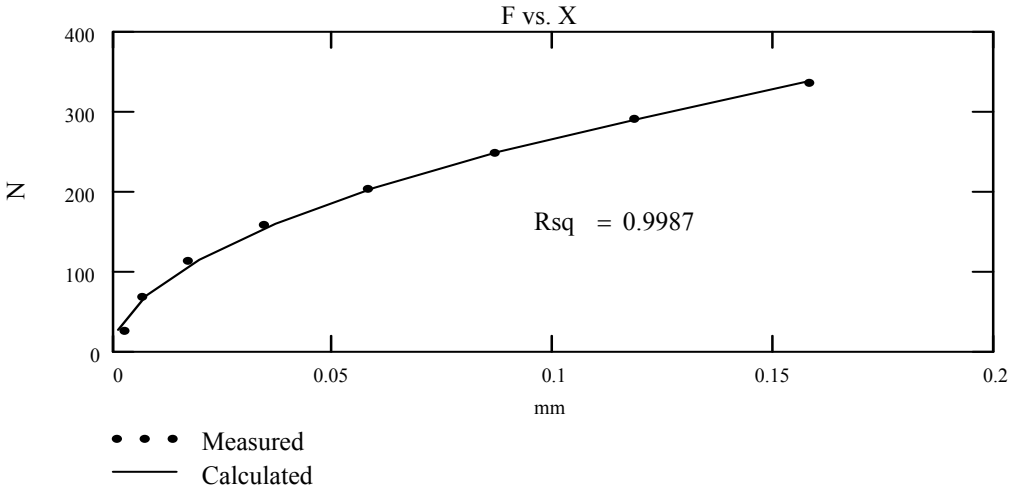

Figure A5 Comparison of measured and calculated (SS Model) force-displacement data

Coefficients are assumed to increase with axial thickness since an axially thick element requires a larger shaker force than an axially thin element (same OD & ID) to achieve a certain radial strain. The relationship is assumed to be linear in the stick-slip model, which would further simplify the design process.

APPENDIX C: MATHCAD WORKSHEET FOR EXTRACTION OF COEFFICIENTS

d1 := "C:\vvc\testing\Mathcad\\Analyze\TRAC1.TXT" dat1 := READPRN(d1)

d2 := "C:\vvc\testing\Mathcad\\Analyze\TRAC2.TXT" dat2 := READPRN(d2)

d3 := "C:\vvc\testing\Mathcad\\Analyze\TRAC3.TXT" dat3 := READPRN(d3)

d4 := "C:\vvc\testing\Mathcad\\Analyze\TRAC4.TXT" dat4 := READPRN(d4)

d5 := "C:\vvc\testing\Mathcad\\Analyze\TRAC5.TXT" dat5 := READPRN(d5)

d6 := "C:\vvc\testing\Mathcad\\Analyze\TRAC6.TXT" dat6 := READPRN(d6)

d7 := "C:\vvc\testing\Mathcad\\Analyze\TRAC7.TXT" dat7 := READPRN(d7)

$i := 0..400$ $f_i := \frac{i}{2}$

$p := 0, 1..350$ $t := 25, 26..375$

$tt_t := t \cdot 3.142$

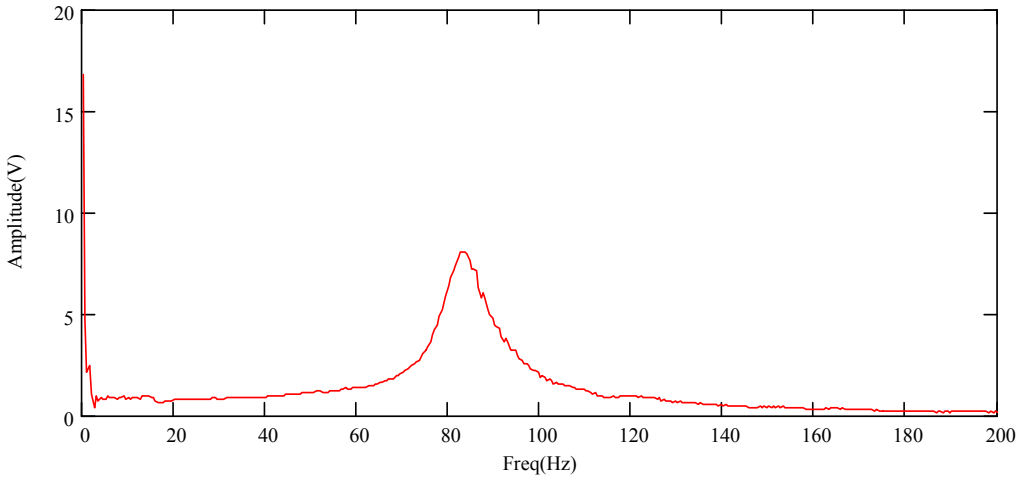

$$amp_i := dat1_i \cdot \frac{.04402}{197.5 \cdot 1.64} \qquad real_i := dat4_i \cdot \frac{.04402}{.1975} \qquad img_i := dat5_i \cdot \frac{.04402}{.1975}$$

$$disp_i := \frac{dat6_i}{197.5} \qquad force_i := dat7_i \cdot 0.04402$$

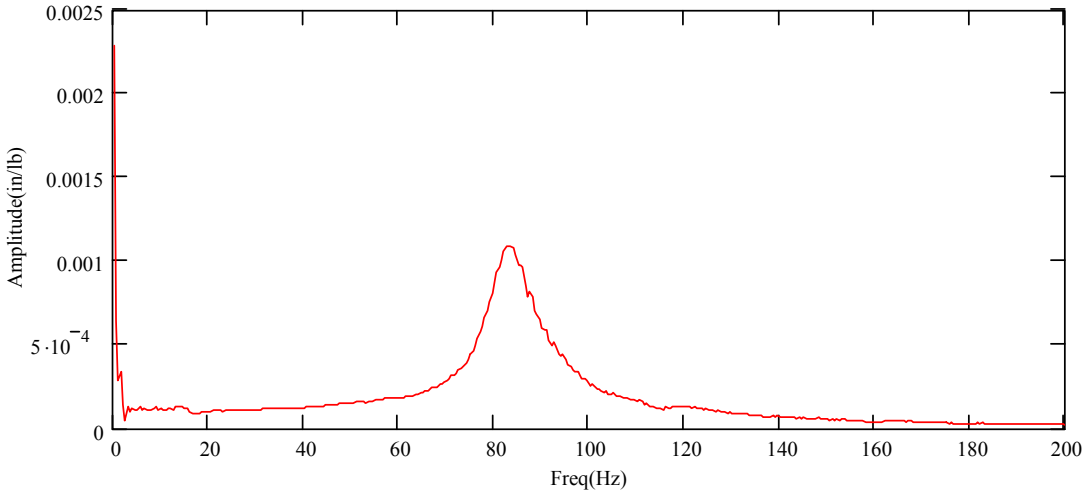

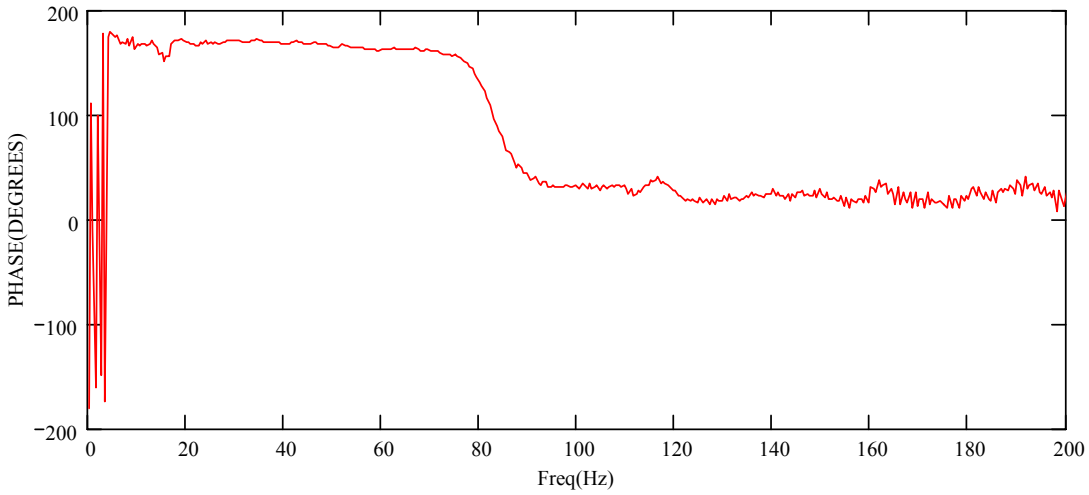

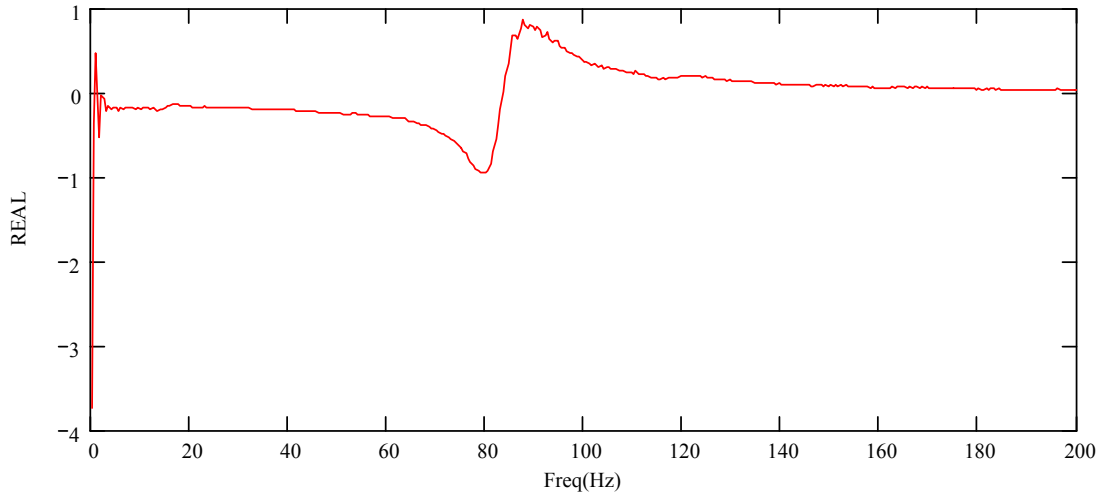
REAL
1
0
−1
−2
−3
−4
0
20
40
60
80
100
120
140
160
180
200
Freq(Hz)

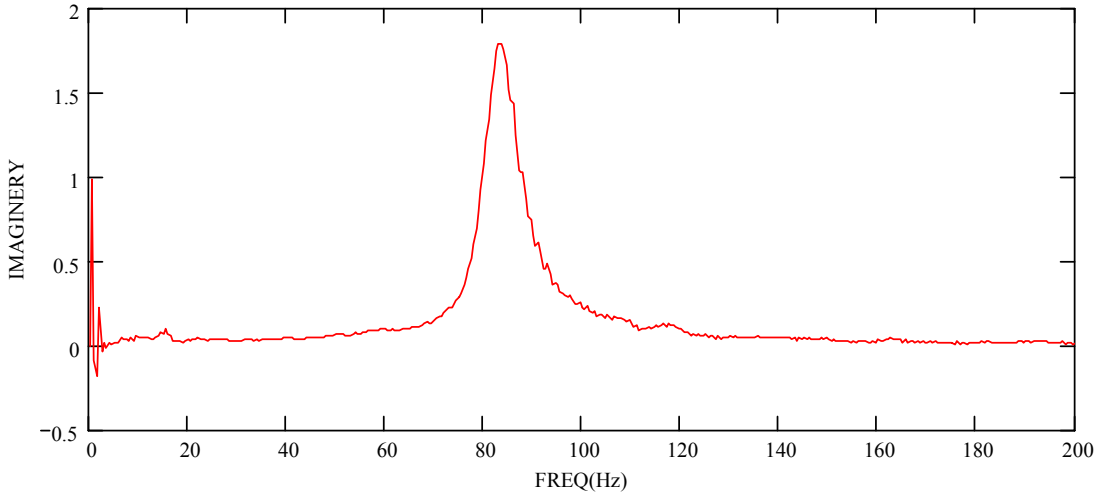
IMAGINERY
2
1.5
1
0.5
0
−0.5
0
20
40
60
80
100
120
140
160
180
200
FREQ(Hz)

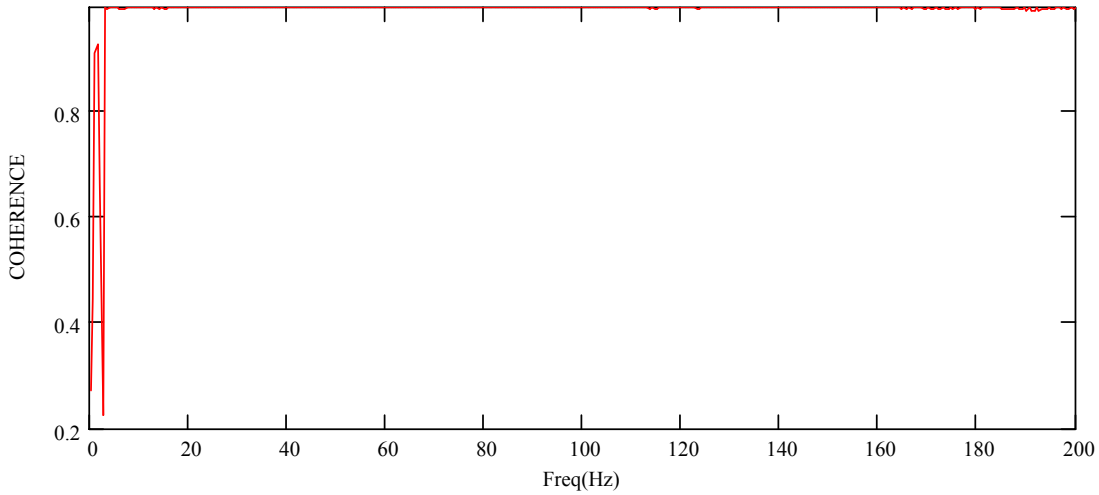
COHERENCE
0.8
0.6
0.4
0.2
0
20
40
60
80
100
120
140
160
180
200
Freq(Hz)

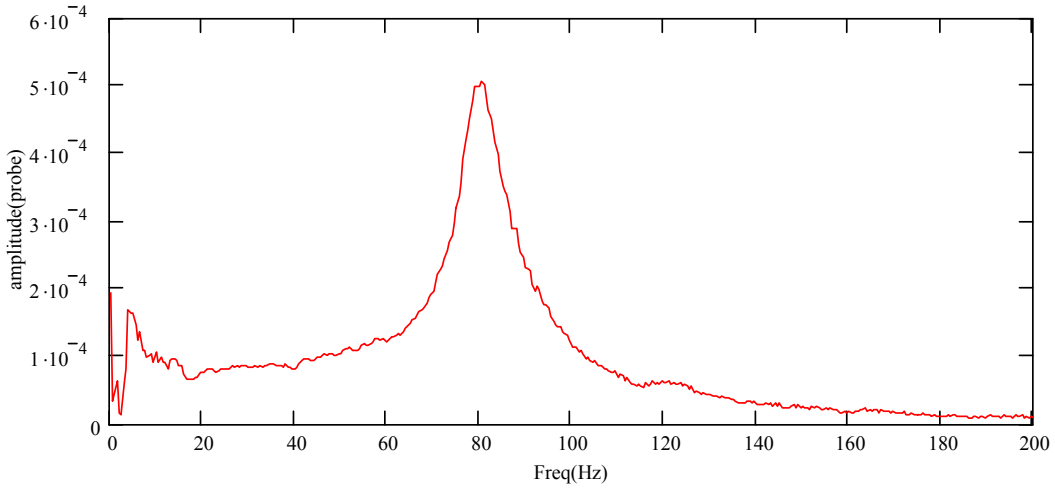

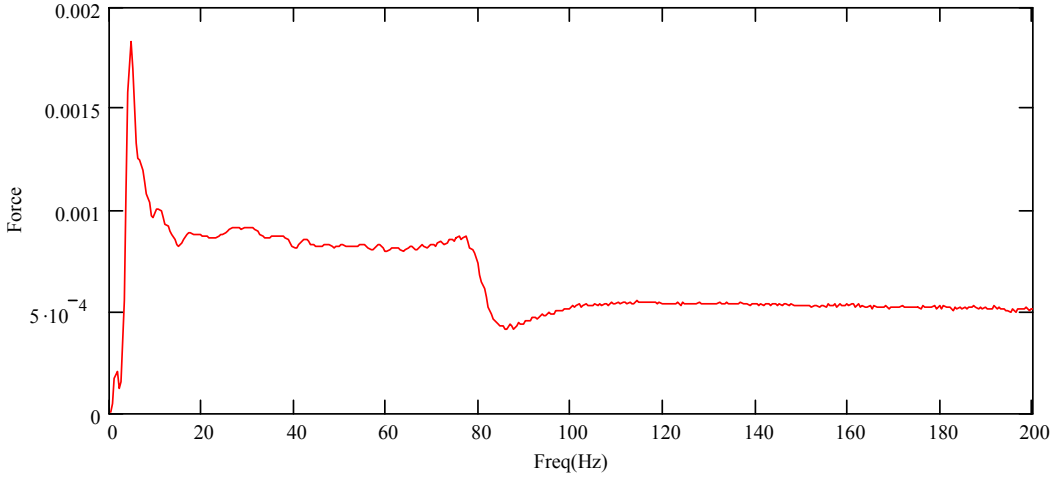

CURVE FITTING BY MATHCAD REGRESSION

$x_t := amp_t$

$$guess := \begin{pmatrix} 30 \times 10^3 \\ 0.025 \\ 10 \end{pmatrix}$$

K

M

C

Initial guess of coefficients to be used in the nonlinear regression method below

$$FF(\omega, u) := \begin{bmatrix} \left[\left(u_0 - u_1\cdot\omega^2\right)^2 + \left(u_2\cdot\omega\right)^2\right]^{\frac{-1}{2}} \\ \frac{-1}{2}\cdot\left[\left(u_0 - u_1\cdot\omega^2\right)^2 + \left(u_2\cdot\omega\right)^2\right]^{\frac{-3}{2}}\cdot\left(2\cdot u_0 - 2\cdot u_1\cdot\omega^2\right) \\ \frac{-1}{2}\cdot\left[\left(u_0 - u_1\cdot\omega^2\right)^2 + \left(u_2\cdot\omega\right)^2\right]^{\frac{-3}{2}}\cdot\left(2\cdot u_1\cdot\omega^4 - 2\cdot u_0\cdot\omega^2\right) \\ \frac{-1}{2}\cdot\left[\left(u_0 - u_1\cdot\omega^2\right)^2 + \left(u_2\cdot\omega\right)^2\right]^{\frac{-3}{2}}\cdot\left(2\cdot u_2\cdot\omega^2\right) \end{bmatrix}$$

Nonlinear regression vector; equations of function and derevatives with respect to each parameter

$$coef := genfit(tt, x, guess, FF)$$

$$coef = \begin{pmatrix} 9.698\times 10^3 \\ 0.035 \\ -1.71 \end{pmatrix}$$

The resulting Coefficients: $Knr := |coef_0|$ $Mnr := |coef_1|$ $c2 := |coef_2|$

$$Hnr_t := \left[\left[Knr - Mnr\cdot(\pi\cdot t)^2\right] + i\left[c2\cdot(\pi\cdot t)\right]\right]$$

90 DEGREE PHASE METHOD

$$aa := \begin{pmatrix} 50 \\ 5 \end{pmatrix}$$

```
la :=  for kk ∈ 25.. 220
         if (|dat2_kk − 90| < aa_1)
           aa_1 ← |dat2_kk − 90|
           aa_0 ← kk/2
       aa
```

$$la = \begin{pmatrix} 83.5 \\ 0.298 \end{pmatrix}$$

$ni := (2la)_0$ $\quad ff := la_0$ $\quad amplitude := \frac{1}{amp_{ni,0}}$ $\quad amplitude = 917.967$

$damping := \frac{amplitude}{3.142 \cdot ni}$ $\quad damping = 1.749$

$k := \frac{1}{amp_{31,0}}$ $\quad k = 8.667 \times 10^3$ lb/in

$mass := \frac{k}{(ff \cdot 2 \cdot 3.142)^2}$ $\quad x_t := amp_{t,0}$ $\quad damping = 1.749$ lb-s/in

$Hnr90_t := \left[\left[k - mass \cdot (\pi \cdot t)^2\right] + i\left[damping \cdot (\pi \cdot t)\right]\right]$ $\quad mass = 0.031$ lb-s^2/in

$\xi 1 := \frac{damping}{2(k \cdot mass)^{0.5}}$

$\xi 1 = 0.053$

AVERAGE

$Knr = 9.698 \times 10^3$ lb/in

$Ka := \frac{Knr}{2} + \frac{k}{2}$ $\quad Ka = 9.182 \times 10^3$ $\quad Kb := Ka - 3510.1$ $\quad Kb = 5.672 \times 10^3$

$c2 = 1.71$ lb-s/in

$Ca := c2$ $\quad Ca = 1.71$ $\quad Cb := Ca - 0.14$ $\quad Cb = 1.57$

$Mnr = 0.035$ lb-s^2/in

$\xi 2 := \frac{c2}{2(Knr \cdot Mnr)^{0.5}}$ $\quad ma := \frac{mass}{2} + \frac{Mnr}{2}$ $\quad ma = 0.033$ $\quad \xi b := \frac{Cb}{2(Kb \cdot ma)^{0.5}}$

$\xi 2 = 0.047$ $\quad \xi a := \frac{\xi 1}{2} + \frac{\xi 2}{2}$ $\quad \xi a = 0.05$ $\quad \xi b = 0.057$

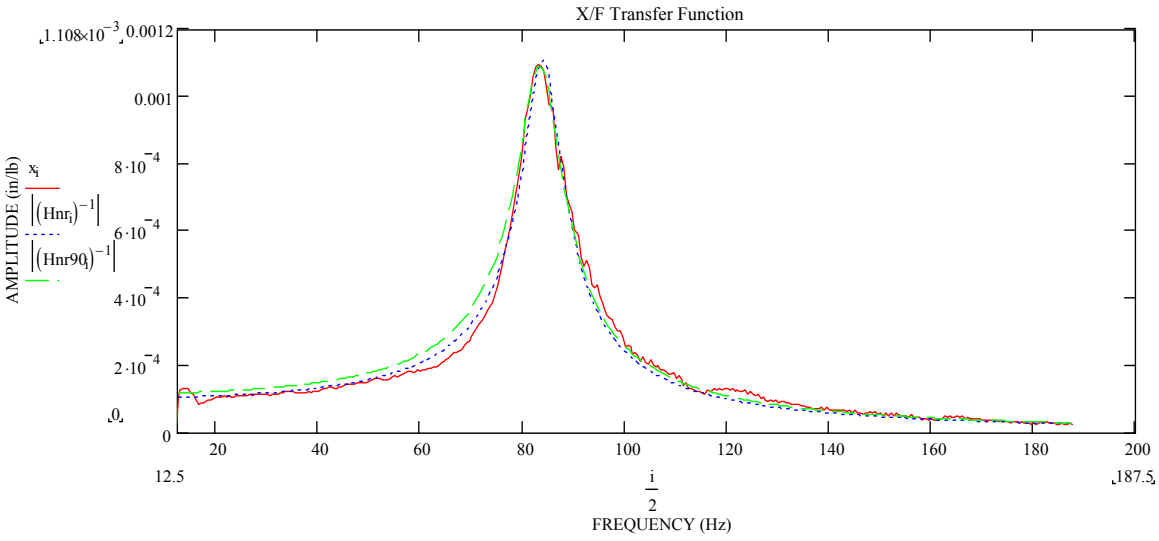

VITA

VIVEK VAIBHAV CHOUDHRY

Address GPS, Indrapuram, PO Majra, Dehradun 248001, India.

Education MS Mechanical Engineering, Texas A&M University, College Station. (08/2002- 08/2004)
Bachelor of Engineering, Regional Engineering College, Allahabad, India. (07/1998-07/2002)

Experience **Research Assistant**, **Turbomachinery Laboratory, Texas A&M University, College Station, TX**. (10/2002 – 8/2004)

- Devised a novel procedure in the form of an EXCEL spreadsheet for calculating the exact pressures in labyrinth/damper seals having multiple blades, which were later utilized, for calculating the rotordynamic coefficients needed in various applications.
- Developed a new method for quantifying the Internal Friction using ADRE, MathCAD and modeling in XLTRC2 towards the fulfillment of TRC project. Designed a new test rotor for ensuring the repeatability of tests for Internal Friction.
- Analyzed the feasibility of using Wire Mesh and Straight seals together as a damping element in an existing test rig using computer simulation and modeling in XLTRC2.
- Working towards Master's thesis on Experimental Evaluation of Wire Mesh as a Damper material. Conducted rigorous tests for quantifying various parameters affecting the rotordynamic coefficients of the Wire Mesh.

Intern, Bharat Heavy Electrical Limited, Hardwar, India
(05/2001 to 08/2001)
Worked in one of the largest producers of turbines in Asia as a team leader motivating a group of six interns in turbine blade shop. Assessed the feasibility of manufacturing turbine blades of long span using the existing machine tools.

Academic Projects

- Lead a group of four students towards designing of a five-speed gearbox for an automobile. Developed the software and the relevant database for the above design of gearbox. Worked on subsequent automation of the gearbox.
- Developed and assembled a model for a straight roll mill and performed stress analysis on the members.

Computer Skills

Visual Basic, C++, MathCAD, MATLAB, AutoCAD, Solidworks, XLTRC2.